

Multiple Choice Learning of Low Rank Adapters for Language Modeling

Victor Letzelter^{* 1 2}

Hugo Malard^{* 1}

Mathieu Fontaine¹

Gaël Richard¹

Slim Essid¹

Andrei Bursuc²

Patrick Pérez³

¹ LTCI, Télécom Paris, Institut Polytechnique de Paris

² Valeo.ai

³ Kyutai

Abstract

We propose LoRA-MCL, a training scheme that extends next-token prediction in language models with a method designed to decode diverse, plausible sentence continuations at inference time. Traditional language modeling is an intrinsically ill-posed problem: given a context, multiple futures may be equally plausible. Our approach leverages Multiple Choice Learning (MCL) and the Winner-Takes-All (WTA) loss to efficiently handle ambiguity through Low-Rank Adaptation (LoRA). We provide a theoretical interpretation of applying Multiple Choice Learning to Language Modeling, assuming the data is generated from a mixture of distributions. To illustrate the proposed approach, we use data sampled from mixtures of Markov chains. We then demonstrate with extensive experiments on real-world visual and audio captioning tasks that our method achieves high diversity and relevance in generated outputs.

1 Introduction

Predicting what a person will say next or describing the content of an audio or visual scene with text is difficult, if not impossible, to do with perfect accuracy. When the context is not informative enough, external factors may lead to different scenarios or *modes* of plausible text continuations [81, 8, 50]. In such ambiguous tasks, the conditional distribution over the space of output sentences given the input context may be multi-modal due to the underlying inherent uncertainty [45].

Initially proposed for text processing, transformer-based language models have quickly become a general framework for modeling streams of tokens, which can also represent, for instance, images and audio signals [68, 6, 38]. Such models are trained as next-token predictors and allow, by nature, for addressing this uncertainty, by generating plausible output sentences through a wide body of maximum a posteriori (MAP) or sampling-based decoding approaches [75]. While sampling allows exploration and diversity, it may lead to unreliable responses and requires truncation to avoid unexpected answers, partly due to the overestimation of low-probability tokens [83, 21]. When seeking reliable and expected answers, maximum a posteriori estimation techniques, like Beam Search [41], look for sentences that maximize the model’s likelihood. However, these alternatives have drawbacks as they may lack diversity, be prone to repetition loops [29], and may sound unnatural [22]. Some approaches, e.g., Diverse Beam Search (DBS) [71], were therefore proposed to artificially increase the diversity at inference, e.g., through a diversity penalty parameter λ , to find a tradeoff

^{*}Equal Contribution.

between generation quality and sample diversity [66]. In contrast with these methods, our approach aims to *predict* diverse sentences reflecting the ambiguity of the input context.

Multiple Choice Learning (MCL) [18, 34] has emerged as a paradigm for addressing ambiguous tasks. It generally consists of a network with a shared backbone and multiple output heads. During training, it utilizes the winner-takes-all loss for adaptively updating the head that performs the best for each example. This is a competitive training scheme that specializes each model to subsets of the conditional output distribution [61, 36]. In this paper, we propose incorporating this idea for language model finetuning, leveraging multiple Low-Rank Adapters [24] instead of multiple heads, which may be impractical due to computation requirements and architectural constraints. Our method natively generates diverse and plausible sequences in a single forward pass, aiming to best approximate the conditional output distribution.

Our contributions are as follows:

We propose a new paradigm that adapts MCL for token sequence modeling, with a method, LoRA-MCL, that is particularly suited for efficient finetuning of language models.

We provide a theoretical analysis of our approach, which applies MCL to language modeling. Assuming the sequences are sampled from a mixture of distributions, we explain in particular why LoRA-MCL should enable capturing the modes of the data distribution. We then consider the case of Markov chains, for which we validate our claims with a well-designed toy example.

We undertake an extensive experimental study to validate our approach, on audio and machine vision captioning tasks, demonstrating its wide applicability in challenging real-world scenarios and showing an excellent diversity–quality trade-off. The code will be made publicly available.

2 Problem setup

Let $x \triangleq (x_t)_{t=1}^T \in \mathcal{V}^T$ be a sequence of T tokens belonging to a finite vocabulary $\mathcal{V} = \{1, \dots, |\mathcal{V}|\}$, and $c \triangleq (c_t)_{t=1}^\tau \in (\mathbb{R}^d)^\tau$ be a sequence of τ context vector embeddings of dimension d . Language modeling aims at learning the law $p(x | c) = \prod_{t=1}^T p(x_t | x_{<t}, c)$ using a model p_θ with parameters θ , by minimizing the following negative log-likelihood loss, which is equivalent to the maximum likelihood estimation (MLE):

$$\mathcal{L}(\theta) = -\mathbb{E}_{c,x}[\log p_\theta(x | c)] = \mathbb{E}_{c,x} \left[-\sum_{t=1}^T \log p_\theta(x_t | x_{<t}, c) \right], \quad (1)$$

where $x_{<t}$ denotes the sequence of tokens prior to time t .

Optimizing (1) is referred to as *teacher-forcing* [77], where p_θ is fed with target (instead of predicted) tokens $x_{<t}$ during training [67]. When using a transformer architecture [69], this is implemented with causal attention modules, which allow for computing the conditional distributions in parallel through all time steps within a single forward pass.

During inference, decoding methods [75] proceed to generating sequences \hat{x} from the trained model p_θ in an auto-regressive fashion. First, they start with a conditional distribution for the first token from the context: $p_\theta(x_1 | c)$, which allows selecting \hat{x}_1 . Then, for $t \geq 2$ they predict $p_\theta(x_t | \hat{x}_{<t}, c)$, and select \hat{x}_t , until reaching either the sequence length limit or an end-of-sentence (EOS) token. The choice of the decoding method used to generate K candidate sequences $\hat{x}^1, \dots, \hat{x}^K$ depends on the purpose of the task, but the general goal is (i) to get highly likely sentences, i.e., ones that maximize $p_\theta(\hat{x})$; and (ii) to get sufficiently diverse sentences, as can be measured by n -gram similarity [25].

Although this is a widely adopted paradigm, we show next how this training and decoding pipeline can be improved: instead of *artificially* generating diversity at inference time, we aim at *learning* to *predict* sequences $\hat{x}^1, \dots, \hat{x}^K$ that cover well the modes of the target distribution $p(x | c)$.

3 Methodology

3.1 Motivation

In language modeling, topic models [53, 5, 8] are data-generating processes in which the ground-truth probability distribution of sequences is modeled as a mixture of latent components or topics. For example, the sequence “I am eating ...” may have multiple plausible continuations, but the likelihood of each depends heavily on contextual factors such as the speaker’s location, which influences their culinary habits. Each location (or context) can thus be associated with a distinct word distribution. In topic models, data generation proceeds by first sampling a topic $z \in \mathcal{Z}$ for each sentence (usually referred to as a *document* in the literature), and then sampling words (or n -grams) from the distribution associated with that topic.

With this in mind, MLE in (1) may not be suitable [81]. While MLE is effective for estimating the overall distribution $p(x)$, it does not capture the individual components when $p(x)$ is expressed as a mixture, i.e., $p(x) = \sum_k p(z_k)p(x|z_k)$. In such cases, MLE tends to model the aggregate rather than distinguish topic-specific distributions $p(x|z_k)$.

3.2 Applying Multiple Choice Learning to language modeling

Our approach is inspired by the multiple choice learning (MCL) literature [18, 34]. We propose the following training scheme, intending to enable the recovery of the different topics z_k . Instead of a single model, we consider a *set* of models $(\theta_1, \dots, \theta_K)$. Then the objective (1) is replaced by one consisting of iterating between the following two steps:

1. For each training sample (c, x) in the batch \mathcal{B} : Compute $p(x|c; \theta_k)$ for $k \in \{1, \dots, K\}$, and choose the best model $k^*(x, c) = \operatorname{argmax}_k p(x|c; \theta_k)$.
2. Compute the winner-takes-all (WTA) loss as:

$$\mathcal{L}^{\text{WTA}}(\theta_1, \dots, \theta_K) = -\mathbb{E}_{c,x} \left[\max_{k=1, \dots, K} \log p(x|c; \theta_k) \right], \quad (2)$$

where $\log p(x|c; \theta_k) = \sum_{t=1}^T \log p(x_t|x_{<t}, c; \theta_k)$, and perform an optimization step.

In practice when using a finite batch size, (2) is approximated with

$$\mathcal{L}^{\text{WTA}}(\theta_1, \dots, \theta_K) \simeq - \sum_{k=1}^K \sum_{\{(x,c) \in \mathcal{B} \mid k^*(x,c)=k\}} \log p(x|c; \theta_k), \quad (3)$$

where each hypothesis k is trained only on the subset of examples in which it is the *winner*, according to the assignment $k^*(x, c)$.

This training procedure, similar to a hard-EM style optimization [52, 76], is a competitive training scheme that encourages the different models to explore different areas of the data distribution. However, it is subject to two main issues: First, using K models instead of a single one drastically increases the training time and memory cost, which may be intractable for large language models. Second, the optimization may be subject to collapse, where the same models are chosen as winners through the iterations, leaving the other models untrained. In the next section, we describe how we solve these issues with our approach LoRA-MCL.

3.3 LoRA-MCL method

Multiple choice learning typically alleviates the high training cost issue of K models by training a single model with several heads [34, 33]. However, we argue that such an approach is not well-suited for fine-tuning language models. First, heads of most language models are quite large (for example in Qwen2-Audio [6] the `1m_head` has $d \times |\mathcal{V}| = 4096 \times 156032 \simeq 640\text{M}$ params), and standard MCL would not scale easily with the number of heads. Second, the initialization of the heads poses several challenges. Initializing each head with the parameters of the head of the pretrained model requires special care, as the collapse of the predictions is likely given the very similar hypotheses (same parameters). A complete re-initialization of the heads is detrimental to performance, as numerous training iterations would be necessary to reach the same level of knowledge as in the pretrained

head. For these reasons, we consider a Low Rank Adapter (LoRA) approach [24] due to its excellent trade-off between performance and computational requirements, as well as its wide adoption in the context of large model fine-tuning.

Let θ be the parameters of the pretrained base model. At each layer ℓ where LoRA is enabled, we use a family of adapters $(A_\ell^k, B_\ell^k) \in \mathbb{R}^{d \times r} \times \mathbb{R}^{r \times d}$ for $k \in \{1, \dots, K\}$. Let

$$\theta_k = \theta \cup \{(A_\ell^k, B_\ell^k) \mid \ell = 1, \dots, L\}, \quad (4)$$

be the set of parameters that are involved in hypothesis k , with L being the total number of layers where LoRA is used.

Training in the WTA fashion involves computing $p(x \mid c; \theta_k)$ for $k = 1, \dots, K$. To avoid collapse into a single head, we may use a (relaxed) winner-takes-all loss as a training objective:

$$\mathcal{L}^{\text{WTA}}(\theta) = -\mathbb{E}_{c,x} \left[\sum_{k=1}^K q_k \log p(x \mid c; \theta_k) \right], \quad (5)$$

where $\{q_k\}$ is a set of coefficients that sum to 1 and that give more weight to the winner index q_{k^*} than to the others, but still provides gradient weight to non-winner heads in order to avoid collapse. In practice, we use $q_{k^*} = 1 - \varepsilon$ and $q_k = \frac{\varepsilon}{K-1}$ for $k \neq k^*$ as in [61].

3.4 Accelerating LoRA-MCL training with parallelization over the hypotheses

A naive implementation of MCL for winner selection, as in Section 3.2, may require a loop over the K hypotheses in the batch to determine the winner associated with each index of the batch, which would drastically slow down training.

To alleviate this issue, we propose the following methodology. Let $\mathbf{x} \in \mathbb{R}^{b \times \mathcal{T} \times d}$ denote the input of the transformer architecture, where b is the batch size, $\mathcal{T} \triangleq T + \tau$ is the total sequence length, and d is the number of features. We duplicate \mathbf{x} , K times along the batch size dimension to get $\mathbf{x}' = (\mathbf{x}_1, \dots, \mathbf{x}_K) \in \mathbb{R}^{bK \times \mathcal{T} \times d}$.

LoRA units at layer ℓ are then computed as:

$$\begin{bmatrix} \mathbf{x}_1 \\ \mathbf{x}_2 \\ \vdots \\ \mathbf{x}_K \end{bmatrix} \leftarrow \begin{bmatrix} B_\ell^1 A_\ell^1 & 0 & 0 & 0 \\ 0 & B_\ell^2 A_\ell^2 & 0 & 0 \\ \vdots & \vdots & \ddots & \vdots \\ 0 & 0 & 0 & B_\ell^K A_\ell^K \end{bmatrix} \begin{bmatrix} \mathbf{x}_1 \\ \mathbf{x}_2 \\ \vdots \\ \mathbf{x}_K \end{bmatrix} + \begin{bmatrix} f_\theta^\ell(\mathbf{x}_1) \\ f_\theta^\ell(\mathbf{x}_2) \\ \vdots \\ f_\theta^\ell(\mathbf{x}_K) \end{bmatrix}, \quad (6)$$

where f_θ^ℓ is the base model (whose parameters remain frozen during training). In practice, this computation is conducted using a Group Convolution operation.¹ While this duplication virtually multiplies the batch size by K , the memory overhead remains manageable, assuming that $r \ll d$. The next section is dedicated to the inner properties of the proposed approach.

4 Theoretical Analysis

We justify the use of MCL in the context of language modeling by assuming that the sequence distribution can be expressed as a mixture. We contrast this formulation with standard maximum likelihood estimation (1). In particular, Section 4.1 establishes a connection between our approach and the Expectation-Maximization (EM) algorithm and derives lower and upper bounds on the optimal achievable test loss. We then apply this analysis to the case of Markov chains in Section 4.2, where the dynamic of the method is simulated in a controlled setting in Section 4.3.

¹This can be done by first reshaping \mathbf{x}' to shape $(b \times \mathcal{T} \times Kd)$ and applying a `nn.Conv1d(Kd, Kd, kernel_size=1, groups=K)` following the PyTorch layer implementation, reshaping back \mathbf{x}' to shape $(Kb \times \mathcal{T} \times d)$ before adding the base model output, and then repeating at the next LoRA unit.

4.1 Training dynamics and optimality conditions

For the next-token prediction loss (1), one can show that: $\min_{\theta} \mathcal{L}(\theta) = \mathcal{H}(x | c)$, where $\mathcal{H}(x | c) \triangleq -\mathbb{E}_{c,x}[\log p(x | c)]$ is the entropy of p [42]. Following the rationale of Section 3.1, let us now assume the data distribution can be written as a mixture. In the case of the WTA loss under this setup, we have the following proposition.

Proposition 1. *Assume the data-generating process is $p(x | c) = \sum_{k=1}^K p(z_k | c) p(x | z_k, c)$ (Asm. 2) with the number of modes equal to the number of hypotheses. Also assume perfect model expressiveness (Asm. 1), and large enough batch size to approximate the true risk well (Asm. 3). Then:*

- (i) *The Winner-Takes-All two-step optimization in LoRA-MCL acts as a conditional form of the hard-EM algorithm.*
- (ii) *Under Assumption 4, and assuming (with one permutation) that $p(x | z_k, c) = p(x | c; \theta_k)$ for each k , $\mathcal{L}^{\text{WTA}}(\theta) = -\mathbb{E}_{x,c} \left[\max_{k=1,\dots,K} \log p(x | c, z_k) \right]$. In this case, we also have:*

$$\mathcal{L}^{\text{WTA}}(\theta) = \mathcal{H}(x | c, z) \triangleq \mathbb{E}_c \left[\sum_{k=1}^K p(z_k | c) \mathcal{H}(x | c, z_k) \right], \quad (7)$$

where $\mathcal{H}(x | c, z)$ is the conditional entropy given the random variable z .

- (iii) *We have the following inequalities:*

$$\min_{\theta} \mathcal{L}(\theta) - \log K \stackrel{(a)}{\leq} \min_{\theta} \mathcal{L}^{\text{WTA}}(\theta) \stackrel{(b)}{\leq} \mathcal{H}(x | c, z) \stackrel{(c)}{\leq} \min_{\theta} \mathcal{L}(\theta), \quad (8)$$

where $\min_{\theta} \mathcal{L}(\theta) = \mathcal{H}(x | c)$.

Proof. See Appendix B. □

(i) in Proposition 1 describes the relationship between LoRA-MCL and the hard-EM algorithm. (ii) provides an expression for the WTA loss as a conditional entropy, $\mathcal{H}(x | c, z)$, under the assumption of a perfect matching between the hypotheses and the modes. Proposition 1 also establishes in (iii) both a lower and an upper bound on the optimal achievable loss for LoRA-MCL, given in (a) and (b), respectively. Note that the gap between these bounds is $\mathcal{H}(x | c, z) - \min_{\theta} \mathcal{L}(\theta) + \log K = -\mathbb{E}_c[\mathcal{I}(x, z | c)] + \log K$ where \mathcal{I} denotes the mutual information. Finally, (c) shows in particular that $\min_{\theta} \mathcal{L}^{\text{WTA}}(\theta) \leq \min_{\theta} \mathcal{L}(\theta)$.

4.2 Case of Markov chains

To make the analysis more concrete, we consider the case where the sequence of tokens is generated from Markov chains. Formally, given a finite state space \mathcal{V} , a homogeneous Markov chain is defined by an initial distribution π over \mathcal{V} and a transition matrix $P \in [0, 1]^{\mathcal{V} \times \mathcal{V}}$. A sequence (x_1, \dots, x_T) is sampled from the Markov chain if $x_1 \sim \pi$ and, for each $t \geq 1$, the conditional distribution of x_{t+1} given x_t is $x_{t+1} | x_t \sim P_{x_t, \cdot}$, where $P_{i,j} = \mathbb{P}(x_{t+1} = j | x_t = i)$. In the following, we ignore the initial warm-up phase and we assume that π is the stationary distribution of P , i.e., such that $\pi P = \pi$. In this case, we will denote $x \sim \text{MC}(P)$.

While the study of the training dynamics of transformers on Markov Chain data has been investigated in previous works [11, 58, 44, 82], our setup instead considers a **mixture** of Markov chains [17, 28]. Assuming a uniform mixture, the data generating process is $x \sim \frac{1}{K} \sum_{k=1}^K \text{MC}(P_k)$, which is equivalent to:

$$z_k \sim \mathcal{U}(1, \dots, K), \quad x | z_k \sim \text{MC}(P_k). \quad (9)$$

When training a language model on such sequences, we have the following Corollary from Prop. 1, where the context c is ignored for simplicity.

Corollary 1. *As per Assumption 5, let us assume that the data-generating process writes as a uniform mixture of Markov chains of order $n = 1$. We denote as $\hat{P}(\theta) \triangleq (p(x_{t+1} = j | x_t = i))_{i,j}$ the predicted transition matrix when using a language model with parameters θ . Under the same assumptions that in Proposition 1, we have that:*

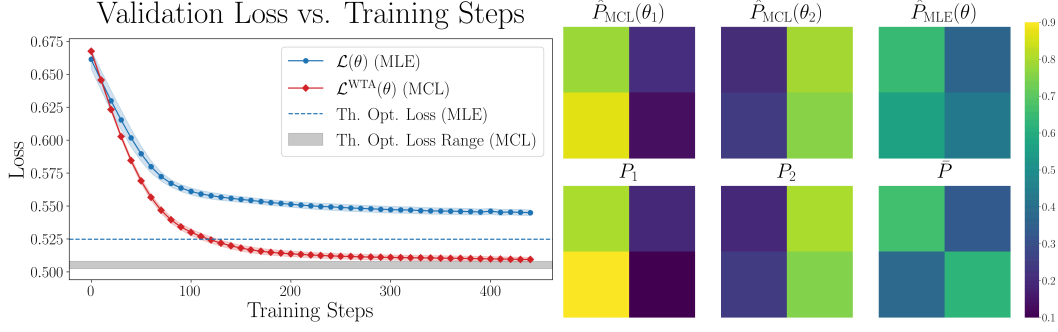


Figure 1: **Comparison of LoRA-MCL with vanilla maximum likelihood estimation (MLE).** The experimental setup is detailed in Section 4.2. (Left) Validation loss over training steps (averaged across three random seeds) for LoRA-MLE (blue) and LoRA-MCL (red). The theoretical optimal MLE loss, approximated via Monte Carlo sampling, is given by the entropy $\mathcal{H}(x)$. The gray shaded region represents the lower and upper bounds of the theoretical optimal MCL loss, as given by (a) and (b) in (8). (Right) Learned transition matrices (top) are compared with the references (bottom). MLE converges approximately toward the weighted average \bar{P} defined as the right-hand side of (10). In contrast, LoRA-MCL successfully recovers the two underlying modes.

- (i) Whenever the maximum likelihood estimator trained with next-token-prediction (12) reaches its optimal loss $\mathcal{L}(\theta)$, we have

$$\hat{P}(\theta)_{i,j} = \frac{1}{\sum_{s=1}^K (\pi_s)_i} \sum_{k=1}^K (\pi_k)_i (P_k)_{i,j}, \quad (10)$$

where $\pi_k \in [0, 1]^{\mathcal{V}}$ is the stationary distribution of P_k .

- (ii) The inequality (8) holds in this context, where the conditional entropy $\mathcal{H}(x|z)$ can be computed by weighting the entropy rate of each Markov Chain:

$$\mathcal{H}(x|z) = -T \sum_{k=1}^K \sum_{i=1}^{|\mathcal{V}|} (\pi_k)_i \left[\sum_{j=1}^{|\mathcal{V}|} (P_k)_{i,j} \log(P_k)_{i,j} \right]. \quad (11)$$

Proof. See Appendix C. □

The entropy $\mathcal{H}(x)$, which is theoretical optimal loss of the MLE baseline, can be computed either exactly for short sequences, or approximated, e.g., through Monte-Carlo integration.

Note that we considered first-order Markov chains in our analysis. We expect the properties generalize to higher orders ($n > 1$) by using transition matrices in the form $P \in [0, 1]^{\mathcal{V}^{n+1}}$ where $P_{i_1, \dots, i_{n+1}} = p(x_{t+1} = i_{n+1} | x_t = i_n, \dots, x_{t-n+1} = i_1)$. Please refer to Appendix C for further discussions.

4.3 Illustration with synthetic data

To illustrate our approach, let us evaluate our algorithm on a synthetic dataset, for which results are given in Figure 1. We used $\mathcal{V} = \{1, 2\}$, and $(P_1, P_2) = (P(p_1, q_1), P(p_2, q_2))$, with $P(p, q) \triangleq \begin{bmatrix} 1-p & p \\ q & 1-q \end{bmatrix}$ and $p, q \in [0, 1]$. We sampled data from a mixture of two Markov chains following (9): we generated a sequence by sampling first $k \sim \mathcal{U}\{1, 2\}$ and then P_k . Once P_k was set, we sampled uniformly the initial state, then sampled the Markov chain according to the transition matrix until reaching the maximum sequence length ($T = 32$ here).

We considered a GPT-2-like architecture [56, 4] using local-attention suggested by [44] to improve convergence on Markov chain data. We then trained the model with 1 and 2 hypotheses, using LoRA adapters as described above, 1 hypothesis corresponding to vanilla maximum likelihood estimation. Training details are provided in Appendix D. Figures 1 and 4 show both the evolution of the losses

along training and the predicted transition matrix from the trained models. We see that the optimum is close to being global in this setup. While LoRA-MCL matches can capture the two modes of the mixture, we see that MLE tends to predict the weighted average of the transition matrices given by (10), which is consistent with Prop. 1.

5 Empirical evaluation

We evaluate LoRA-MCL on realistic datasets and large-scale models for audio and image captioning tasks. Predicting a textual description for images or audio signals is an ill-posed problem: from an input image or audio clip, multiple descriptions may be plausible. We argue this is a particularly relevant real-world case of ill-posed problems, where the conditional output distribution is inherently multi-modal. Our goal is to demonstrate that LoRA-MCL provides a competitive approach for capturing these distribution modes when fine-tuning either audio (Sec. 5.2) or vision-language models (Sec. 5.3). We present hereafter the experimental setup. Please refer to Appendix E.2 for further details.

5.1 Experimental Setup

Datasets. We experimented on both Clotho-V2 [14, 10], and AudioCaps [16, 30] datasets for the audio captioning task, while we make use of the TextCaps dataset [65] for a challenging task for vision language models coined as image captioning with reading comprehension. Table 4 of the Appendix describes the datasets sizes.

Architecture and training details with audio data. We used the instructed version of Qwen2-Audio [6] as the base model, which has ~ 8.4 billion parameters and a vocabulary size $|\mathcal{V}| = 156,032$. We used LoRA adapters applied to the Q, K, V linear projections of the attention modules, and the upside and downside projections of the feedforward blocks, for all the layers of the transformers. We used a rank r and scaling factor α , with $r = \alpha = 8$ unless otherwise stated. We trained for 1 epoch on AudioCaps and 10 epochs on Clotho with a validation loss computed at the end of each epoch.

Architecture and training details with visual data. We used LLaVA 1.6 [38] with Vicuna-7B [86] for the LLM, as the base model which features ~ 7.1 billion parameters and a vocabulary size $|\mathcal{V}| = 32,000$. We used the [official codebase](#) for the implementation. Following standard practices [87], we applied LoRA adapters only for the LLM decoder. The adapters were applied to Q, K, V , upside and downside projections as in Qwen2-Audio, and we used $r = \frac{\alpha}{4} = 8$ unless otherwise stated. Training was done over 1 epoch (without validation data), and the validation set of TextCaps was used for evaluation.

Metrics. We evaluate the approach using various quality metrics. First, we compute the test-loss (or perplexity), which evaluates the likelihood of the reference captions under the trained model. Second, we use natural language generation quality metrics (BLEU- n , ROUGE, METEOR) [54, 37, 3] based on n -gram matching between predicted and target sentences. We also leverage the latter proposed CIDEr, SPICE and SPIDEr [70, 1, 39] metrics, which show higher correlation with human evaluation for captioning tasks. Finally, we use Sentence-BERT (sBERT) [60, 88] for embedding comparison. We consider sentence-based oracle evaluation for these metrics (see e.g., [34, Sec. 4.3] or [32]). To evaluate the diversity of the generated captions, we consider: Div- n , which compares the number of distinct n -grams against the number of n -grams for a set of generated captions as in [50] and Self-BLEU (mBLEU-4), which computes BLEU similarity scores between generated captions [89].

Baselines. To validate our approach, we compare it against a maximum likelihood baseline (LoRA-MLE) trained using (1), under the same conditions as the ones considered for our multi-hypothesis model. Specifically, both models use the same LoRA configuration, the same number of trainable parameters (the LoRA rank for the baseline is $K \times$ larger to this end), and the same number of iterations. At inference time, for each decoding method applied to the baseline that returns K sentences, we decode the same number of candidates with LoRA-MCL. When evaluating Maximum A Posteriori methods –greedy, beam search [41] and diverse beam search [71]–, we ensure a consistent computational budget by aligning the number of forward passes. For example, if the MLE baseline uses a beam size of B , our model uses a beam size of $\frac{B}{K}$ per hypothesis.

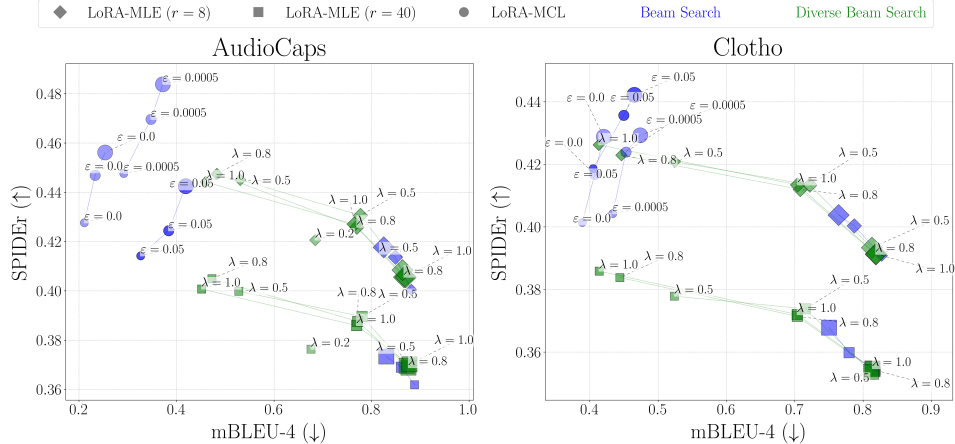


Figure 2: **Quality vs. Diversity on Audio Captioning with 5 candidates.** Quality measured by SPIDEr (↑) and Diversity by mBLEU-4 (↓). Marker shape stands for the method, and size is proportional to the number of forwards performed per example at inference time. Note that LoRA-MLE was trained with two rank values, $r = 8$ and $r = 8K$, for fair comparison in terms of parameter count. Color corresponds to the decoding method (beam search or diverse beam search). Values of ε and λ for LoRA-MCL and diverse beam search, resp., are indicated in the plot, with the color shade proportional to the corresponding parameter value to better distinguish the markers.

5.2 Audio captioning

Quality vs. diversity trade-off. Quality–diversity performance is shown in Figure 2. While a well-chosen value of λ allows Diverse Beam Search applied to LoRA-MLE to be competitive, LoRA-MCL (circles) achieves the best trade-off between quality and diversity, appearing in the top-left corner of the plot. Although increasing the beam size generally improves performance for standard beam search, we observe that increasing the beam size within each group negatively impacts Diverse Beam Search. In theory, setting $\varepsilon = 0$ should maximize both quality and diversity. However, using a small positive value of ε ensures all heads are trained, albeit at the cost of reduced diversity and potentially quality when ε is too large. Full results are given in Tables 5 and 6 of the Appendix.

Effect of the number of hypotheses. We include in Figures 6 and 5 (given in the appendix) the same plot as in Figure 2, but using 3 and 4 candidates, respectively. These results further reinforce the findings obtained with 5 hypotheses. In Table 1, we report the evolution of the test negative log-likelihood (NLL) loss as a function of the number of hypotheses, showing a monotonically decreasing trend. This provides additional evidence for Proposition 1, and shows that LoRA-MCL improves its coverage of the data distribution modes as K increases.

Table 1: **Test Loss (↓) as a function of the number of hypotheses K .** LoRA-MCL is trained with $\varepsilon = 0.05$ and $r = 8$.

Training	K	AudioCaps	Clotho
LoRA-MLE ($r = 8$)	1	2.152	2.811
LoRA-MLE ($r = 40$)	1	2.124	2.902
LoRA-MCL	2	2.071	2.700
LoRA-MCL	3	2.021	2.665
LoRA-MCL	5	1.927	2.629
LoRA-MCL	8	1.869	2.592

5.3 Image description with reading comprehension

5.3.1 Quality and Diversity Evaluation

Similarly to Figure 2, Table 2 confirms the trends observed in the audio captioning task. At an equal number of forward passes, LoRA-MCL outperforms LoRA-MLE, even using DBS decoding with a λ diversity parameter specifically optimized for the task (SPIDEr of 0.955 against 0.915). However, we noticed that the DBS decoding of LoRA-MLE tends to generate more diverse outputs than the greedy decoding of LoRA-MCL (mBLEU of 0.416 against 0.520). Interestingly, increasing the number of beams in each group decreases diversity and does not improve the performance of LoRA-MLE, while with LoRA-MCL, increasing the beam size (from 1 to 2) not only slightly increases the performance

Table 2: **Quality and Diversity Evaluation on TextCaps with 3 candidates.** Best scores are in **bold**, second-best are underlined. For each of the presented metrics, higher is better (\uparrow) except for mBLEU-4 (\downarrow). LoRA-MCL is trained with $\varepsilon = 0.1$, $r = 8$ and $\alpha = 32$. LoRA-MLE is trained with $r = 24$ and $\alpha = 4 \times r = 96$, ensuring the same dynamics and number of parameters across models. For completeness, we also trained LoRA-MLE with $r = 8$ and $\alpha = 32$ in the rows marked with \dagger .

Training	Decoding	Beam	mBLEU-4	BLEU-4	METEOR	sBERT	CIDEr-D	SPICE	SPIDEr
LoRA-MLE	Beam Search	3	0.688	0.318	0.315	0.670	1.517	0.244	0.873
LoRA-MLE	Beam Search	6	0.786	0.338	0.326	0.671	1.557	0.246	0.895
LoRA-MLE	DBS ($\lambda = 0.8$)	3	0.437	0.349	0.327	0.686	1.590	0.251	0.909
LoRA-MLE	DBS ($\lambda = 1.0$)	3	0.416	0.348	0.326	0.685	1.586	0.250	0.906
LoRA-MLE †	DBS ($\lambda = 1.0$)	3	0.425	0.357	0.327	0.686	1.601	0.252	0.915
LoRA-MLE	DBS ($\lambda = 0.8$)	6	0.671	0.341	0.328	0.681	1.573	0.251	0.903
LoRA-MLE	DBS ($\lambda = 1.0$)	6	0.666	0.340	0.328	0.680	1.577	0.250	0.904
LoRA-MLE †	DBS ($\lambda = 1.0$)	6	0.671	0.341	0.328	0.680	1.584	0.251	0.908
LoRA-MCL	Beam Search	1	0.520	0.344	<u>0.330</u>	0.690	1.674	<u>0.255</u>	0.955
LoRA-MCL	Beam Search	2	0.490	0.360	0.333	<u>0.687</u>	<u>1.627</u>	0.258	<u>0.932</u>

but also improves the diversity of the generations, indicating promising further inference-time scaling. Additional results are provided in Appendix (Table 9).

5.3.2 Observing hypothesis specialization in bilingual image description

To highlight the behavior of LoRA-MCL in a realistic case where one can control the modes of the data-generating process, we simulated an artificial bi-modal distribution of the dataset, similarly to the setup of the toy experiment of Section 4.3. We did so by translating half of the captions of the data from English to French (using T5-small [57]), while keeping the prompts in English.

We trained and evaluated a 2-hypothesis model in the LoRA-MCL setup, as well as a baseline trained in LoRA-MLE. We observed a clear specialization of each hypothesis towards a given language (i.e., one hypothesis learned French and the other English): at test-time, the winning head is the first one in $\sim 89\%$ of the French captions and the second one in $\sim 97\%$ of the English captions. Table 3 shows performance and diversity scores of both LoRA-MLE and LoRA-MCL on our synthetic test set. LoRA-MCL is decoded greedily while LoRA-MLE uses DBS with the λ value maximizing its performance (0.8). Although the overall performances are similar, LoRA-MCL generates significantly more diverse captions (mBLEU-4 of 0.027 and 0.029 against 0.138 and 0.126 on the French and English subparts, respectively), and outperforms LoRA-MLE in the French part of the test set (SPIDEr of 0.464 against 0.411).

These results relate to the synthetic data experiments of Sec. 4.2: in the presence of two modes, LoRA-MLE learns an average of them. Here, we believe this is more shifted toward English as the original LLaVA model performs better in English than in French. In contrast, LoRA-MCL is expected to learn the two modes separately. We believe this is what explains the gain in performance in French, at the cost of a slight reduction in English performance.

Fig. 3 qualitatively illustrates the behavior of the models: LoRA-MLE learns a weighted average of the two modes, shifted towards English, and it is sometimes not able to output French captions within the 2 candidates as in the book example. We found LoRA-MLE to be particularly prone to errors when outputting French sentences: for instance, in the second generation of examples with an image of a bottle, LoRA-MLE enters a repetition loop. On the other hand, LoRA-MCL is less affected by those artifacts on French sentences, and successfully captures the two modes of the distribution, benefiting from the specialization of each hypothesis.

6 Related Work

Multiple Choice Learning to predict diverse and plausible outputs. Multiple Choice Learning [18, 34] is a training paradigm that minimizes the *oracle* or *winner-takes-all* loss across a set of models, encouraging specialization [61, 36]. While it has been noted that the collapse issue needs to be addressed with care [61, 55], MCL has demonstrated broad applicability across machine learning tasks [33, 62, 15], typically using a shared backbone and multiple projection heads. However, using

Table 3: **SPIDER** (\uparrow) & **mBLEU-4** (\downarrow) on different parts of synthetic test set.

Test subset	Training	SPIDER	mBLEU-4
French	LoRA-MLE	0.411	0.138
	LoRA-MCL	0.464	0.027
English	LoRA-MLE	0.756	0.126
	LoRA-MCL	0.722	0.029



LoRA-MLE.
 {A bottle of Cerveza is on a table.}
 {Une bouteille de vin de cidre de cidre de cidre [...]}

LoRA-MCL.
 {A bottle of beer with a label that says "Sel Maguet"}
 {Une bouteille de vin est étiquetée avec le mot « Maguay ».}



LoRA-MLE.
 {A book titled Papa Told Me is being held by a person.}
 {A book called Papa told me is being held by a person.}

Lora-MCL.
 {A book titled Papa Told Me is being held by a person}
 {Un livre papier intitulé Papa Told Me.}

Figure 3: **Observing specialization in bilingual image description.** Quantitative (*Left*) and Qualitative (*Right*) analysis for LoRA-MLE and LoRA-MCL in the setup of Section 5.3.2.

multiple heads may be impractical in large language models. Mixture-of-Experts [26, 63] can be an effective strategy to manage computational costs in this case. However, as primarily thought for model scalability and not diversity, only a small subset of experts are active at each forward pass via routing, making them incompatible with MCL, while still suffering from knowledge redundancy in the experts [27]. To the best of our knowledge, we are the first to adapt MCL to the setup of language modeling with next-token prediction, specifically, using internal models instantiated via multiple LoRA [24].

Generating Multiple Outputs with Language Models. Language models are commonly trained via next-token prediction, framed as Maximum Likelihood Estimation. This is arguably the most popular method for training large-scale language models [64, 56, 68], including those that take audio or images as input [6, 38], with much of its success attributed to tokenization [44, 58]. Generating diverse and plausible sequences at inference remains challenging: (i) Sampling methods [22, 13, 51] may be unreliable depending on the chosen parameters; (ii) Exact MAP decoding is intractable due to the exponential search space [12]; (iii) Strategies like Beam Search often yield repetitive or overly coherent outputs [13, 22, 29]. Diverse Beam Search [50] or contrastive decoding [66] inject diversity through test-time parameters (e.g., penalty λ), but in contrast, our method infers diversity from the input’s inherent ambiguity.

Diversity in Audio and Visual Captioning. Audio [9, 48, 49] and image captioning [2, 20, 23] have traditionally relied on dataset- and task-specific models trained with Maximum Likelihood Estimation (MLE). A key challenge identified in both domains is the lack of diversity in generated captions, prompting the development of other training objectives specifically designed to address this issue [50, 80, 79, 84, 72, 73, 43]. These methods often require architectural modifications and are typically designed for models trained from scratch. However, recent advances have shifted the field toward general-purpose multimodal large language models [6, 38], which offer broader capabilities but pose new challenges to address the diversity-quality trade-off. In this work, we demonstrate that LoRA-MCL can be effectively applied at the fine-tuning stage of such models.

7 Conclusion

This paper proposes a new paradigm for training language models to generate diverse plausible predictions. This is done with LoRA-MCL, combining the Multiple Choice Learning paradigm and Low-rank Adaptation. We provide a theoretical analysis showing that when the target sequence is written as a mixture, LoRA-MCL is expected to capture the modes of the data distribution. We validate our analysis with experiments on Markov chains, and on the real-world audio and advanced image captioning tasks. Future work includes a careful interpretation of the concepts learned by each model as a function of the ambiguity of the input, e.g., for uncertainty estimation as an alternative to [74].

Limitations. In LoRA-MCL, setting ε too high ensures that all hypotheses receive gradients, but it can also overly homogenize the models, thereby reducing diversity. While MCL performs well across a broad range of ε values, identifying the optimal setting can be challenging. To do so, we plan to incorporate recent annealing MCL techniques, e.g., [55], which employ a scheduling mechanism for ε and may help improve the quality of the solution. Note that recent LoRA variants, such as [19] may also be an orthogonal axis of improvement for our method.

Acknowledgments

We thank Mickael Chen for his valuable advice, as well as Gilles Puy for his help in the implementation of the parallelization over the hypotheses. This work was funded by the French Association for Technological Research (ANRT CIFRE contract 2022-1854), and granted access to the HPC resources of IDRIS (allocation 2024-AD011014345) by GENCI.

References

1. Peter Anderson, Basura Fernando, Mark Johnson, and Stephen Gould. Spice: Semantic propositional image caption evaluation. In *ECCV*, 2016. 7
2. Jyoti Aneja, Aditya Deshpande, and Alexander G Schwing. Convolutional image captioning. In *CVPR*, 2018. 10
3. Satyanjeev Banerjee and Alon Lavie. Meteor: An automatic metric for mt evaluation with improved correlation with human judgments. In *ACL Workshops*, 2005. 7
4. Sid Black, Leo Gao, Phil Wang, Connor Leahy, and Stella Biderman. GPT-Neo: Large Scale Autoregressive Language Modeling with Mesh-Tensorflow, March 2021. 6, 20
5. David M Blei, Andrew Y Ng, and Michael I Jordan. Latent dirichlet allocation. *JMLR*, 2003. 3
6. Yunfei Chu, Jin Xu, Qian Yang, Haojie Wei, Xipin Wei, Zhifang Guo, Yichong Leng, Yuanjun Lv, Jinzheng He, Junyang Lin, et al. Qwen2-audio technical report. *arXiv preprint arXiv:2407.10759*, 2024. 1, 3, 7, 10, 21
7. Thomas M Cover. *Elements of information theory*. John Wiley & Sons, 1999. 20
8. Adji B Dieng, Francisco JR Ruiz, and David M Blei. Topic modeling in embedding spaces. *TACL*, 2020. 1, 3
9. Konstantinos Drossos, Sharath Adavanne, and Tuomas Virtanen. Automated audio captioning with recurrent neural networks. In *WASPAA*, 2017. 10
10. Konstantinos Drossos, Samuel Lipping, and Tuomas Virtanen. Clotho: An audio captioning dataset. In *ICASSP*, 2020. 7, 21, 22
11. Ezra Edelman, Nikolaos Tsilivis, Benjamin Edelman, Eran Malach, and Surbhi Goel. The evolution of statistical induction heads: In-context learning markov chains. *NeurIPS*, 2024. 5
12. Bryan Eikema and Wilker Aziz. Is map decoding all you need? the inadequacy of the mode in neural machine translation. In *COLING*, 2020. 10
13. Angela Fan, Mike Lewis, and Yann Dauphin. Hierarchical neural story generation. In *ACL*, 2018. 10
14. Frederic Font, Gerard Roma, and Xavier Serra. Freesound technical demo. In *ACMMM*, 2013. 7, 21
15. Nuno Cruz Garcia, Sarah Adel Bargal, Vitaly Ablavsky, Pietro Morerio, Vittorio Murino, and Stan Sclaroff. Distillation multiple choice learning for multimodal action recognition. In *WACV*, 2021. 9
16. Jort F Gemmeke, Daniel PW Ellis, Dylan Freedman, Aren Jansen, Wade Lawrence, R Channing Moore, Manoj Plakal, and Marvin Ritter. Audio set: An ontology and human-labeled dataset for audio events. In *ICASSP*, 2017. 7, 21
17. Rishi Gupta, Ravi Kumar, and Sergei Vassilvitskii. On mixtures of markov chains. *NeurIPS*, 2016. 5
18. Abner Guzman-Rivera, Dhruv Batra, and Pushmeet Kohli. Multiple choice learning: Learning to produce multiple structured outputs. *NeurIPS*, 2012. 2, 3, 9

19. Soufiane Hayou, Nikhil Ghosh, and Bin Yu. Lora+: Efficient low rank adaptation of large models. *ICML*. 10
20. Simao Herdade, Armin Kappeler, Kofi Boakye, and Joao Soares. Image captioning: Transforming objects into words. *NeurIPS*, 2019. 10
21. John Hewitt, Christopher D Manning, and Percy Liang. Truncation sampling as language model desmoothing. In *EMNLP*, 2022. 1
22. Ari Holtzman, Jan Buys, Li Du, Maxwell Forbes, and Yejin Choi. The curious case of neural text degeneration. In *ICLR*, 2019. 1, 10
23. MD Zakir Hossain, Ferdous Sohel, Mohd Fairuz Shiratuddin, and Hamid Laga. A comprehensive survey of deep learning for image captioning. *ACM Computing Surveys (CSUR)*, 2019. 10
24. Edward J Hu, Yelong Shen, Phillip Wallis, Zeyuan Allen-Zhu, Yuanzhi Li, Shean Wang, Lu Wang, Weizhu Chen, et al. Lora: Low-rank adaptation of large language models. In *ICLR*, 2022. 2, 4, 10
25. Daphne Ippolito, Reno Kriz, João Sedoc, Maria Kustikova, and Chris Callison-Burch. Comparison of diverse decoding methods from conditional language models. In *ACL*, 2019. 2
26. Robert A Jacobs, Michael I Jordan, Steven J Nowlan, and Geoffrey E Hinton. Adaptive mixtures of local experts. *Neural computation*, 1991. 10
27. Albert Q Jiang, Alexandre Sablayrolles, Antoine Roux, Arthur Mensch, Blanche Savary, Chris Bamford, Devendra Singh Chaplot, Diego de las Casas, Emma Bou Hanna, Florian Bressand, et al. Mixtral of experts. *arXiv preprint arXiv:2401.04088*, 2024. 10
28. Chinmaya Kausik, Kevin Tan, and Ambuj Tewari. Learning mixtures of markov chains and mdps. In *ICML*, 2023. 5
29. Nitish Shirish Keskar, Bryan McCann, Lav R Varshney, Caiming Xiong, and Richard Socher. Ctrl: A conditional transformer language model for controllable generation. *arXiv preprint arXiv:1909.05858*, 2019. 1, 10, 21, 24
30. Chris Dongjoo Kim, Byeongchang Kim, Hyunmin Lee, and Gunhee Kim. Audiocaps: Generating captions for audios in the wild. In *NAACL*, 2019. 7, 21, 22
31. Etienne Labb, Thomas Pellegrini, Julien Pinquier, et al. Conette: An efficient audio captioning system leveraging multiple datasets with task embedding. *TASLPRO*, 2024. 21
32. Etienne Labbé, Thomas Pellegrini, and Julien Pinquier. Is my automatic audio captioning system so bad? spider-max: a metric to consider several caption candidates. In *DCASE*, 2022. 7
33. Kimin Lee, Changho Hwang, KyoungSoo Park, and Jinwoo Shin. Confident multiple choice learning. In *ICML*, 2017. 3, 9
34. Stefan Lee, Senthil Purushwalkam Shiva Prakash, Michael Cogswell, Viresh Ranjan, David Crandall, and Dhruv Batra. Stochastic multiple choice learning for training diverse deep ensembles. In *NeurIPS*, 2016. 2, 3, 7, 9
35. Victor Letzelter, Mathieu Fontaine, Mickaël Chen, Patrick Pérez, Slim Essid, and Gaël Richard. Resilient multiple choice learning: A learned scoring scheme with application to audio scene analysis. In *NeurIPS*, 2023. 18
36. Victor Letzelter, David Perera, Cédric Rommel, Mathieu Fontaine, Slim Essid, Gaël Richard, and Patrick Perez. Winner-takes-all learners are geometry-aware conditional density estimators. In *ICML*, 2024. 2, 9
37. Chin-Yew Lin. Rouge: A package for automatic evaluation of summaries. In *Text summarization branches out*, 2004. 7
38. Haotian Liu, Chunyuan Li, Qingyang Wu, and Yong Jae Lee. Visual instruction tuning. In *NeurIPS*, 2023. 1, 7, 10

39. Siqi Liu, Zhenhai Zhu, Ning Ye, Sergio Guadarrama, and Kevin Murphy. Improved image captioning via policy gradient optimization of spider. In *ICCV*, 2017. 7
40. Ilya Loshchilov and Frank Hutter. Decoupled weight decay regularization. In *ICLR*, 2017. 22, 25
41. Bruce T Lowerre. *The harpy speech recognition system*. Carnegie Mellon University, 1976. 1, 7
42. David JC MacKay. *Information theory, inference and learning algorithms*. Cambridge university press, 2003. 5, 16
43. Shweta Mahajan and Stefan Roth. Diverse image captioning with context-object split latent spaces. *NeurIPS*, 2020. 10
44. Ashok Vardhan Makkuva, Marco Bondaschi, Adway Girish, Alliot Nagle, Martin Jaggi, Hyeji Kim, and Michael Gastpar. Attention with markov: A framework for principled analysis of transformers via markov chains. *arXiv preprint arXiv:2402.04161*, 2024. 5, 6, 10, 20
45. Andrey Malinin and Mark Gales. Uncertainty estimation in autoregressive structured prediction. *ICLR*, 2020. 1
46. Sourab Mangrulkar, Sylvain Gugger, Lysandre Debut, Younes Belkada, Sayak Paul, and Benjamin Bossan. Peft: State-of-the-art parameter-efficient fine-tuning methods. <https://github.com/huggingface/peft>, 2022. 21
47. Geoffrey J McLachlan, Sharon X Lee, and Suren I Rathnayake. Finite mixture models. *Annual review of statistics and its application*, 2019. 18
48. Xinhao Mei, Xubo Liu, Qiushi Huang, Mark D Plumbley, and Wenwu Wang. Audio captioning transformer. In *DCASE*, 2021. 10
49. Xinhao Mei, Xubo Liu, Mark D Plumbley, and Wenwu Wang. Automated audio captioning: An overview of recent progress and new challenges. *EURASIP*, 2022. 10
50. Xinhao Mei, Xubo Liu, Jianyuan Sun, Mark D Plumbley, and Wenwu Wang. Diverse audio captioning via adversarial training. In *ICASSP*, 2022. 1, 7, 10
51. Clara Meister, Tiago Pimentel, Gian Wiher, and Ryan Cotterell. Locally typical sampling. *TACL*, 2023. 10
52. Sewon Min, Danqi Chen, Hannaneh Hajishirzi, and Luke Zettlemoyer. A discrete hard em approach for weakly supervised question answering. In *EMNLP-IJCNLP*, 2019. 3
53. Kamal Nigam, Andrew Kachites McCallum, Sebastian Thrun, and Tom Mitchell. Text classification from labeled and unlabeled documents using em. *ML*, 2000. 3
54. Kishore Papineni, Salim Roukos, Todd Ward, and Wei-Jing Zhu. Bleu: a method for automatic evaluation of machine translation. In *ACL*, 2002. 7
55. David Perera, Victor Letzelter, Théo Mariotte, Adrien Cortés, Mickael Chen, Slim Essid, and Gaël Richard. Annealed multiple choice learning: Overcoming limitations of winner-takes-all with annealing. In *NeurIPS*, 2024. 9, 10
56. Alec Radford, Jeffrey Wu, Rewon Child, David Luan, Dario Amodei, Ilya Sutskever, et al. Language models are unsupervised multitask learners. *OpenAI blog*, 1(8):9, 2019. 6, 10, 20
57. Colin Raffel, Noam Shazeer, Adam Roberts, Katherine Lee, Sharan Narang, Michael Matena, Yanqi Zhou, Wei Li, and Peter J Liu. Exploring the limits of transfer learning with a unified text-to-text transformer. *MLR*, 2020. 9, 25
58. Nived Rajaraman, Jiantao Jiao, and Kannan Ramchandran. An analysis of tokenization: Transformers under markov data. In *NeurIPS*, 2024. 5, 10
59. Richard A Redner and Homer F Walker. Mixture densities, maximum likelihood and the em algorithm. *SIAM review*, 1984. 18

60. N Reimers. Sentence-bert: Sentence embeddings using siamese bert-networks. *arXiv preprint arXiv:1908.10084*, 2019. 7
61. Christian Rupprecht, Iro Laina, Robert DiPietro, Maximilian Baust, Federico Tombari, Nassir Navab, and Gregory D Hager. Learning in an uncertain world: Representing ambiguity through multiple hypotheses. In *ICCV*, 2017. 2, 4, 9
62. Younggyo Seo, Kimin Lee, Ignasi Clavera Gilaberte, Thanard Kurutach, Jinwoo Shin, and Pieter Abbeel. Trajectory-wise multiple choice learning for dynamics generalization in reinforcement learning. In *NeurIPS*, 2020. 9
63. Noam Shazeer, Azalia Mirhoseini, Krzysztof Maziarczyk, Andy Davis, Quoc Le, Geoffrey Hinton, and Jeff Dean. Outrageously large neural networks: The sparsely-gated mixture-of-experts layer. In *ICLR*, 2017. 10
64. Buck Shlegeris, Fabien Roger, Lawrence Chan, and Euan McLean. Language models are better than humans at next-token prediction. *TMLR*, 2022. 10
65. Oleksii Sidorov, Ronghang Hu, Marcus Rohrbach, and Amanpreet Singh. Textcaps: a dataset for image captioning with reading comprehension. In *ECCV*, 2020. 7, 22
66. Yixuan Su and Nigel Collier. Contrastive search is what you need for neural text generation. *TMLR*, 2023. 2, 10
67. Ilya Sutskever, Oriol Vinyals, and Quoc V Le. Sequence to sequence learning with neural networks. In *NeurIPS*, 2014. 2
68. Hugo Touvron, Thibaut Lavril, Gautier Izacard, Xavier Martinet, Marie-Anne Lachaux, Timothée Lacroix, Baptiste Rozière, Naman Goyal, Eric Hambro, Faisal Azhar, et al. Llama: Open and efficient foundation language models. *arXiv preprint arXiv:2302.13971*, 2023. 1, 10
69. Ashish Vaswani, Noam Shazeer, Niki Parmar, Jakob Uszkoreit, Llion Jones, Aidan N Gomez, Łukasz Kaiser, and Illia Polosukhin. Attention is all you need. In *NeurIPS*, 2017. 2
70. Ramakrishna Vedantam, C Lawrence Zitnick, and Devi Parikh. Cider: Consensus-based image description evaluation. In *CVPR*, 2015. 7
71. Ashwin Vijayakumar, Michael Cogswell, Ramprasaath Selvaraju, Qing Sun, Stefan Lee, David Crandall, and Dhruv Batra. Diverse beam search for improved description of complex scenes. In *AAAI*, 2018. 1, 7
72. Qingzhong Wang and Antoni B Chan. Describing like humans: on diversity in image captioning. In *CVPR*, 2019. 10
73. Qingzhong Wang, Jia Wan, and Antoni B Chan. On diversity in image captioning: Metrics and methods. *IEEE Transactions on Pattern Analysis and Machine Intelligence*, 2020. 10
74. Xi Wang, Laurence Aitchison, and Maja Rudolph. Lora ensembles for large language model fine-tuning. *arXiv preprint arXiv:2310.00035*, 2023. 10
75. Sean Welleck, Amanda Bertsch, Matthew Finlayson, Hailey Schoelkopf, Alex Xie, Graham Neubig, Ilia Kulikov, and Zaid Harchaoui. From decoding to meta-generation: Inference-time algorithms for large language models. *TMLR*, 2024. 1, 2
76. Yuqiao Wen, Yongchang Hao, Yanshuai Cao, and Lili Mou. An equal-size hard EM algorithm for diverse dialogue generation. In *ICLR*, 2023. 3
77. Ronald J Williams and David Zipser. A learning algorithm for continually running fully recurrent neural networks. *Neural computation*, 1989. 2
78. Thomas Wolf, Lysandre Debut, Victor Sanh, Julien Chaumond, Clement Delangue, Anthony Moi, Pierric Cistac, Tim Rault, Rémi Louf, Morgan Funtowicz, et al. Huggingface’s transformers: State-of-the-art natural language processing. *arXiv preprint arXiv:1910.03771*, 2019. 21

79. Manjie Xu, Chenxing Li, Xinyi Tu, Yong Ren, Ruibo Fu, Wei Liang, and Dong Yu. Towards diverse and efficient audio captioning via diffusion models. *arXiv preprint arXiv:2409.09401*, 2024. 10
80. Xuenan Xu, Mengyue Wu, and Kai Yu. Diversity-controllable and accurate audio captioning based on neural condition. In *ICASSP*, 2022. 10
81. Zhilin Yang, Zihang Dai, Ruslan Salakhutdinov, and William W Cohen. Breaking the softmax bottleneck: A high-rank rnn language model. In *ICLR*, 2018. 1, 3
82. Oussama Zekri, Ambroise Odonnat, Abdelhakim Benechehab, Linus Bleistein, Nicolas Boullé, and Ievgen Redko. Large language models as markov chains. *arXiv preprint arXiv:2410.02724*, 2024. 5
83. Hugh Zhang, Daniel Duckworth, Daphne Ippolito, and Arvind Neelakantan. Trading off diversity and quality in natural language generation. In *HumEval*, 2021. 1
84. Yiming Zhang, Ruoyi Du, Zheng-Hua Tan, Wenwu Wang, and Zhanyu Ma. Generating accurate and diverse audio captions through variational autoencoder framework. *IEEE Signal Processing Letters*, 2024. 10
85. Eric Zhao, Pranjal Awasthi, and Sreenivas Gollapudi. Sample, scrutinize and scale: Effective inference-time search by scaling verification. *arXiv preprint arXiv:2502.01839*, 2025. 24
86. Lianmin Zheng, Wei-Lin Chiang, Ying Sheng, Siyuan Zhuang, Zhanghao Wu, Yonghao Zhuang, Zi Lin, Zhuohan Li, Dacheng Li, Eric Xing, et al. Judging llm-as-a-judge with mt-bench and chatbot arena. In *NeurIPS*, 2023. 7
87. Xionghao Zhou, Jie He, Yuhua Ke, Guangyao Zhu, Víctor Gutiérrez-Basulto, and Jeff Z Pan. An empirical study on parameter-efficient fine-tuning for multimodal large language models. In *ACL*, 2024. 7
88. Zelin Zhou, Zhiling Zhang, Xuenan Xu, Zeyu Xie, Mengyue Wu, and Kenny Q Zhu. Can audio captions be evaluated with image caption metrics? In *ICASSP*, 2022. 7
89. Yaoming Zhu, Sidi Lu, Lei Zheng, Jiaxian Guo, Weinan Zhang, Jun Wang, and Yong Yu. Texygen: A benchmarking platform for text generation models. In *SIGIR*, 2018. 7

A Notations and setup

In the following, $x \triangleq (x_t)_{t=1}^T \in \mathcal{V}^T$ be a sequence of T tokens belonging to a finite vocabulary $\mathcal{V} = \{1, \dots, |\mathcal{V}|\}$, and $c \triangleq (c_t)_{t=1}^\tau \in (\mathbb{R}^d)^\tau$ be a sequence of τ context of embeddings of dimension d . In the following $\mathcal{X} = \mathcal{V}^T$ and $\mathcal{C} = (\mathbb{R}^d)^\tau$.

Language modeling aims at learning the law $p(x|c) = \prod_{t=1}^T p(x_t | x_{<t}, c)$ using a model p_θ with parameters $\theta \in \Theta$, by maximum likelihood estimation, minimizing the negative log-likelihood loss

$$\mathcal{L}(\theta) = -\mathbb{E}_{c,x}[\log p_\theta(x|c)] = \mathbb{E}_{c,x} \left[-\sum_{t=1}^T \log p_\theta(x_t | x_{<t}, c) \right], \quad (12)$$

where $x_{<t}$ denotes the sequence of tokens prior to time t . In practice, we assume that $p_\theta = s_\eta \circ f_\theta$, where $f_\theta(x_{<t}, c) \in \mathbb{R}^\mathcal{V}$ are the predicted logits and $s_\eta : z \in \mathbb{R}^\mathcal{V} \mapsto \left(\frac{\exp(z_j/\eta)}{\sum_{q=1}^{|\mathcal{V}|} \exp(z_q/\eta)} \right) \in [0, 1]^\mathcal{V}$ is the softmax operator with temperature $\eta > 0$.

In the following, we make the following assumption.

Assumption 1 (Expressiveness). *In the following, we assume that the model p_θ is perfectly expressive. Formally, let $\mathcal{F}_\theta \triangleq \{p_\theta : \mathcal{C} \rightarrow \mathcal{P}(\mathcal{X})\}$ be the family of conditional distributions realized by the model, where $\mathcal{P}(\mathcal{X})$ is the set of probability distributions on \mathcal{X} . We assume the family \mathcal{F}_θ is perfectly expressive, that is $\mathcal{F}_\theta = \{p^* : \mathcal{C} \rightarrow \mathcal{P}(\mathcal{X})\}$.*

First, note that we have the Proposition 2, a well-known result that is due to the Gibbs inequality (e.g., [42]), for which we provide a proof for completeness.

Proposition 2 ([42]). *Under Assumption 1, for the next-token prediction loss (12), one can show that*

$$\min_\theta \mathcal{L}(\theta) = \mathcal{H}(x|c), \quad (13)$$

where $\mathcal{H}(x|c) \triangleq -\mathbb{E}_{c,x}[\log p(x|c)]$ is the entropy of $p(\cdot|c)$.

Proof. Let us denote $\mathcal{S}(p) = \{(x, c) | p(x, c) > 0\}$ the support of p . We use the convention $p(x, c) \log p(x, c) = 0$ for $(x, c) \in \mathcal{X} \times \mathcal{C} - \mathcal{S}(p)$. Because log is a concave function, we have under Jensen's inequality:

$$-\int_{\mathcal{S}(p)} \log \left[\frac{p_\theta(x|c)}{p(x, c)} \right] p(x, c) \, dx dc \geq -\log \left(\int_{\mathcal{S}(p)} \frac{p_\theta(x|c)}{p(x, c)} p(x, c) \, dx dc \right) \geq 0. \quad (14)$$

However, because of the convention, the left-hand side of (14) is also equal to the integral over $\mathcal{X} \times \mathcal{C}$. This shows:

$$-\int_{\mathcal{X} \times \mathcal{C}} p(x, c) \log p_\theta(x|c) \, dx dc \geq -\int_{\mathcal{X} \times \mathcal{C}} p(x, c) \log p(x|c) \, dx dc = \mathcal{H}(x|c),$$

where the equality is reached for parameter θ such that $p_\theta = p$, whose existence is guaranteed by Assumption 1. \square

In the following, we denote the Kullback–Leibler divergence between two distributions α and β as $\text{KL}(\alpha \| \beta) \triangleq \int_{\mathcal{S}(\beta)} \alpha(x) \log \frac{\alpha(x)}{\beta(x)} dx$, where $\mathcal{S}(\beta) \triangleq \{x \in \mathcal{X} | \beta(x) > 0\}$. Note that we have the equality:

$$-\mathbb{E}_\alpha[\log \beta(x)] = \text{KL}(\alpha \| \beta) + \mathcal{H}(\alpha), \quad (15)$$

where the left-hand side is usually referred as the Cross-Entropy, and $\mathcal{H}(\alpha) \triangleq -\mathbb{E}_\alpha[\log \alpha(x)]$ is the entropy of α . When the context is clear, we will also write the entropy of a distribution α as $\mathcal{H}(x)$ where $x \sim \alpha$.

B Proof of Proposition 1

Let us now consider the following assumptions.

Assumption 2 (Mixture of latent processes). *The data-generating process writes in form $p(x | c) = \sum_{k=1}^K p(z_k | c) p(x | z_k, c)$. The Mixture is said to be uniform if $\forall k, p(z_k | c) = \frac{1}{K}$.*

Assumption 3 (Minimization of the true risk). *The batch size is large enough so that the minimization of the empirical risk comes down to minimizing the true risk (12).*

Remark 1. *Under Assumptions 2 and 3, the optimal reachable loss by maximum likelihood estimation is $\min_{\theta} \mathcal{L}(\theta) = \mathbb{E}_c [\mathcal{H}(x | c)]$, where $x \sim \frac{1}{K} \sum_{k=1}^K p(x | z_k, c)$.*

Assumption 4 (Disjoint components). *This assumption states that $p(x | c, z_s) = 0$ when $p(x | c, z_k) > 0$, for $s \neq k$.*

Proposition 3. *Under Assumptions 1, 2, and 3, we have that:*

(i) *The Winner-Takes-All two-step optimization in LoRA-MCL acts as a conditional form of the hard-EM algorithm.*

(ii) *Under Assumption 4, and assuming (with one permutation) that $p(x | z_k, c) = p(x | c; \theta_k)$ for each k , $\mathcal{L}^{\text{WTA}}(\theta) = -\mathbb{E}_{x,c} \left[\max_{k=1,\dots,K} \log p(x | c, z_k) \right]$. In this case, we also have:*

$$\mathcal{L}^{\text{WTA}}(\theta) = \mathcal{H}(x | c, z) \triangleq \mathbb{E}_c \left[\sum_{k=1}^K p(z_k | c) \mathcal{H}(x | c, z_k) \right], \quad (16)$$

where $\mathcal{H}(x | c, z)$ is the conditional entropy given the random variable z .

(iii) *We have the following inequalities:*

$$\min_{\theta} \mathcal{L}(\theta) - \log K \stackrel{(a)}{\leq} \min_{\theta} \mathcal{L}^{\text{WTA}}(\theta) \stackrel{(b)}{\leq} \mathcal{H}(x | c, z) \stackrel{(c)}{\leq} \min_{\theta} \mathcal{L}(\theta), \quad (17)$$

where $\min_{\theta} \mathcal{L}(\theta) = \mathcal{H}(x | c)$.

Proof of (i) First, let us remind that the hard-EM consists of fitting a distribution $p_{\theta}(x, z)$ to observed data $x \sim p(x)$ where z are (unknown) hidden variables. The fitting starts from randomly initialized parameters θ and latent variables z . It consists of repeating the following operations at each iteration t until convergence:

1. (Expectation) $z_k^* = \operatorname{argmax}_k p(x, z_k; \theta^{(t)})$
2. (Maximization) $\theta^{(t+1)} = \operatorname{argmax}_{\theta} p(x, z_k^*; \theta^{(t)})$

Let us define:

$$D(\theta, q) \triangleq \int_{\mathcal{X}} \sum_{k=1}^K q(k | x) \log p(x, z_k; \theta) \, dp(x), \quad D(\theta) \triangleq \int_{\mathcal{X}} \max_{k=1,\dots,K} \log p(x, z_k; \theta) \, dp(x), \quad (18)$$

where q is a discrete distribution over $\{1, \dots, K\}$ with exactly one non-zero component that controls the assignment of each x to a fixed k^* . Let us define $q(\theta)$ as the discrete distribution defined so that $q(k | x; \theta) \triangleq \mathbf{1}[k = \operatorname{argmax}_s p(x, z_s; \theta)]$. Note that then $D(\theta) = D(\theta, q(\theta))$.

For the vanilla (or soft) EM algorithm, the complete data log-likelihood $\int_{\mathcal{X}} \log p(x; \theta) p(x) dx$ is expected to increase at each iteration t . Similarly, for the hard-EM, we have that the $D(\theta)$ increases at each iteration.

Indeed, the expectation step comes down to computing $q(\theta^{(t)})$. For the Maximization step, we have: $D(\theta^{(t+1)}, q(\theta^{(t)})) \geq D(\theta^{(t)}, q(\theta^{(t)}))$, by definition. At the next expectation step, we have: $D(\theta^{(t+1)}, q(\theta^{(t+1)})) \geq D(\theta^{(t+1)}, q(\theta^{(t)}))$, because $q(\theta^{(t+1)})$ computes the best assignment given the parameters $\theta^{(t+1)}$. This shows that $D(\theta^{(t+1)}) \geq D(\theta^{(t)})$.

First note that the main difference compared to the vanilla form of the (hard) EM algorithm, is that the goal is to fit here a *conditional* distribution $p(x | c)$ given pair $(c, x) \sim p(c, x)$. Furthermore, step 2 performs a gradient step (of the neural network weights) instead of a full maximization.

Note that under Assumption 2 the complete data log-likelihood writes as $\log p(x | c; \theta) = \log \left[\sum_{k=1}^K p(x, z_k | c; \theta) \right]$. However, the variables z_k are not known in practice. Lora-MCL works by analogy with the Hard-EM algorithm, which consists, in the Expectation step, of picking for each pair $(x; c)$, $k^*(x, c) = \arg\max_k p(x | c; \theta_k)$. Indeed, under Assumption 3, each training step of Lora-MCL writes as the optimization of

$$\mathcal{L}^{\text{WTA}}(\theta) = - \int_{\mathcal{X} \times \mathcal{C}} \max_{k=1, \dots, K} \log p(x | c; \theta_k) dp(c, x), \quad (19)$$

which is expected to decrease at each training iteration. Note that because the loss is bounded from below (by 0), the sequence of real numbers $\{\mathcal{L}^{\text{WTA}}(\theta^{(t)})\}_{t \geq 0}$ is therefore expected to converge.

To conclude, we can view $(\theta_1, \dots, \theta_K)$ as the parameters involved in the estimation of the modes of the conditional distribution with $p(x | c) = \sum_{k=1}^K p(x | c; \theta_k) p(\theta_k | c)$. Note that the current form of the algorithm does not estimate the weight of each mode $p(\theta_k | c)$, further work could include incorporating *scoring* heads to estimate $p(\theta_k | c)$ each k as in [35]. \square

We then expect to be able to recover the distributions (with one permutation) $\{p(x | c, z_k)\}$ from estimated $\{p(x | c; \theta_k)\}$, assuming identifiability of the data generating mixture, which we expect to be made easier if the components are enough separated (See e.g., [59, Par. 2.5] or [47, Sec. 2.2]).

Proof of (ii) Let us assume that (with one permutation) $p(x | z_k, c) = p(x | c; \theta_k)$ for $k \in \{1, \dots, K\}$. This is possible thanks to Assumption 1. Let us show that (16).

Let us define:

$$\mathcal{X}_k(c, \theta) \triangleq \left\{ x \in \mathcal{X} \mid \log p(x | c, \theta_k) \geq \log p(x | c, \theta_s) \ \forall s \in \{1, \dots, K\} \right\}. \quad (20)$$

In this case, the WTA loss (2) writes as

$$\begin{aligned} \mathcal{L}^{\text{WTA}}(\theta) &= - \int_{\mathcal{C}} \sum_{k=1}^K \int_{\mathcal{X}_k(c, \theta)} \log p(x | c; \theta_k) p(x | c) dx p(c) dc \\ &= - \int_{\mathcal{C}} \sum_{k=1}^K \sum_{s=1}^K \int_{\mathcal{X}_k(c, \theta)} \log p(x | c; z_k) p(x | c; z_s) p(z_s | c) dx p(c) dc \\ &= - \int_{\mathcal{C}} \sum_{k=1}^K \int_{\mathcal{X}_k(c, \theta)} \log p(x | c; z_k) p(x | c; z_k) p(z_k | c) dx p(c) dc \quad \text{by Asm. 4} \\ &= - \int_{\mathcal{C}} \sum_{k=1}^K \mathcal{H}(x | c; z_k) p(z_k | c) p(c) dx dc \quad \text{as } \int_{\mathcal{X}_k(c, \theta)} p(x | c; z_k) dx = 1. \\ &= \mathbb{E}_c \left[\sum_{k=1}^K p(z_k | c) \mathcal{H}(x | c; z_k) \right]. \end{aligned}$$

\square

Proof of (iii) Let us show that:

$$\min_{\theta} \mathcal{L}(\theta) - \log K \stackrel{(a)}{\leq} \min_{\theta} \mathcal{L}^{\text{WTA}}(\theta) \stackrel{(b)}{\leq} \mathcal{H}(x | c, z) \stackrel{(c)}{\leq} \min_{\theta} \mathcal{L}(\theta).$$

(a): First, we have $\max_{k=1, \dots, K} p(x | c, z_k) \leq \sum_{k=1}^K p(x | c, \theta_k)$. Therefore,

$$\begin{aligned} \mathcal{L}^{\text{WTA}}(\theta) &\geq -\mathbb{E}_{x, c} \left[\log \frac{1}{K} \sum_{k=1}^K p(x | c, \theta_k) \right] - \log K \\ &= \underbrace{\text{KL} \left[p(x | c) \parallel \frac{1}{K} \sum_{k=1}^K p(x | c, \theta_k) \right]}_{\geq 0} + \mathcal{H}(x | c) - \log K \quad \text{by (15)} \\ &\geq \mathcal{H}(x | c) - \log K. \end{aligned}$$

Because $\min_{\theta} \mathcal{L}(\theta) = \mathcal{H}(x|c)$, we have shown that (a) occurs when the KL term vanishes, which is when $p(x|c) = \frac{1}{K} \sum_{k=1}^K p(x|c, \theta_k)$.

(b): We have

$$\begin{aligned} \mathcal{L}^{\text{WTA}}(\theta) &= -\mathbb{E}_x \left[\max_{k=1, \dots, K} \log p(x|c, \theta_k) \right] \\ &= -\mathbb{E}_z \mathbb{E}_x | z \left[\log \frac{\max_{k=1, \dots, K} p(x|c, \theta_k)}{p(x|c, z)} \right] \underbrace{- \mathbb{E}_z \mathbb{E}_x | z [\log p(x|c, z)]}_{\mathcal{H}(x|c, z)}. \end{aligned}$$

Now let us leverage Assumption 1 to choose $\tilde{\theta}_k$ such that $p(x|c, \tilde{\theta}_k) = p(x|c, z_k)$ for each $k \in \{1, \dots, K\}$. In this case, $\max_k p(x|c, \tilde{\theta}_k) \geq p(x|c, z)$ for each $z \in \{z_1, \dots, z_K\}$, and $-\mathbb{E}_z \mathbb{E}_x | z \left[\log \frac{\max_k p(x|c, \tilde{\theta}_k)}{p(x|c, z)} \right] \leq 0$. Then,

$$\min_{\theta} \mathcal{L}^{\text{WTA}}(\theta) \leq \mathcal{L}(\tilde{\theta}_1, \dots, \tilde{\theta}_K) \leq \mathcal{H}(x|c, z),$$

which proves (b).

Finally (c) can be directly deduced from the inequality $\mathcal{H}(x|c, z) \leq \mathcal{H}(x|c)$. \square

C Proof of Corollary 1

Let us consider the following assumptions.

Assumption 5 (Markov Chain). *We assume that the data-generating process writes as a uniform mixture of Markov chains of order $n \in \mathbb{N} \setminus \{0\}$, that is, for each t and each k , $p(x_t | x_{<t}, c, z_k) = p(x_t | x_{t-1}, \dots, x_{t-n}, c, z_k)$.*

Corollary 2. *As per Assumption 5, let us assume that the data-generating process writes as a uniform mixture of Markov chains of order $n = 1$. We denote as $\hat{P}(\theta) \triangleq (p(x_{t+1} = j | x_t = i))_{i,j}$ the predicted transition matrix when using a language model with parameters θ . Under the same assumptions that in Proposition 1, we have:*

- (i) *Whenever the maximum likelihood estimator trained with next-token-prediction (12) reaches its optimal loss $\mathcal{L}(\theta)$, we have*

$$\hat{P}(\theta)_{i,j} = \sum_{k=1}^K p(z = z_k | x_t = i) (P_k)_{i,j} = \frac{1}{\sum_{s=1}^K (\pi_s)_i} \sum_{k=1}^K (\pi_k)_i (P_k)_{i,j},$$

where $\pi_k \in [0, 1]^{\mathcal{V}}$ is the stationary distribution of P_k .

- (ii) *The inequality (8) holds in this context, where the conditional entropy $\mathcal{H}(x|z)$ can be computed by a weighted sum the entropy rate of each of the K Markov Chains:*

$$\mathcal{H}(x|z) = -T \sum_{k=1}^K \sum_{i=1}^{|\mathcal{V}|} (\pi_k)_i \left[\sum_{j=1}^{|\mathcal{V}|} (P_k)_{i,j} \log(P_k)_{i,j} \right].$$

The entropy $\mathcal{H}(x)$, which is the lower bound of the MLE baseline, can be computed either exactly for short sequences, or approximated, e.g., through Monte-Carlo integration.

Proof of (i) The Cross entropy of the maximum-likelihood model is optimal whenever $p_{\theta} = p$.

In this case, for each $i, j \in \{1, \dots, |\mathcal{V}|\}$, we have $p_{\theta}(x_{t+1} = j | x_t = i) = p(x_{t+1} = j | x_t = i)$ and

$$p_{\theta}(x_{t+1} = j | x_t = i) = \sum_{k=1}^K p(z = z_k | x_t = i) p(x_{t+1} = j | x_t = i, z_k). \quad (21)$$

Furthermore, by Bayes' rule, we have:

$$p(z = z_k | x_t = i) = \frac{p(x_t = i | z = z_k) p(z = z_k)}{\sum_{s=1}^K p(x_t = i | z = z_s) p(z = z_s)} = \frac{(\pi_k)_i}{\sum_{s=1}^K (\pi_s)_i},$$

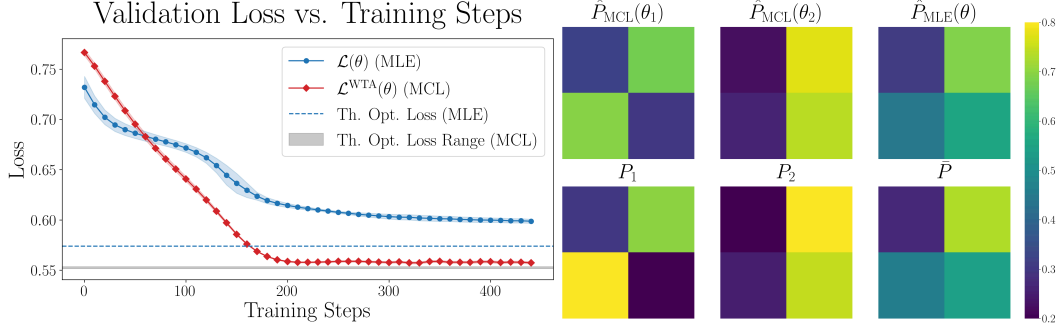


Figure 4: **Comparison of LoRA-MCL with standard maximum likelihood estimation (MLE).** The setup mirrors that of Figure 1, but uses different transition matrices. While the overall behavior remains consistent with Figure 1, we observe a distinct transition in the MLE loss. We interpret this as evidence that MLE increasingly incorporates contextual information as training progresses (see also [44]).

because we have assumed a uniform prior over the mixture components, i.e., $p(z = z_k) = \frac{1}{K}$, and we assumed stationary regime so that $p(x_t = i | z = z_k) = (\pi_k)_i$. \square

Proof of (ii) Because we assumed first-order Markov Chains, we have

$$\mathcal{H}(x) = \sum_{t=1}^T \mathcal{H}(x_t | x_{<t}).$$

Because we assumed stationary Markov chains, we have that $\mathcal{H}(x_t | x_{t-1})$ doesn't depend on t and $\mathcal{H}(x_t | x_{t-1}) = \mathcal{H}(x_2 | x_1) = -\sum_{i=1}^{|\mathcal{V}|} (\pi_k)_i \left[\sum_{j=1}^{|\mathcal{V}|} (P_k)_{i,j} \log(P_k)_{i,j} \right]$ (see [7] page 66, Theorem 4.2.4). \square

Note that we considered first-order Markov chains in our analysis. However we expect the properties to generalize to higher orders ($n > 1$) by using transition matrices in the form $P \in [0, 1]^{V^{n+1}}$ where

$$P_{i_1, \dots, i_{n+1}} = p(x_{t+1} = i_{n+1} | x_t = i_n, \dots, x_{t-n+1} = i_1).$$

D Experimental details of Section 4.3

The results in Figure 1 were obtained using the setup described in this section. The same illustration with different transition matrices is shown in Figure 4. Note that in both figures, the loss and theoretical quantities are normalized by $T - 1$, since the first token is excluded from the computation.

Dataset. We used a uniform mixture of two first-order homogeneous Markov chains with transition matrices $(P_1, P_2) = (P(p_1, q_1), P(p_2, q_2))$, with $P(p, q) \triangleq \begin{bmatrix} 1-p & p \\ q & 1-q \end{bmatrix}$ and $p, q \in [0, 1]$. For the experiment in Figure 1, we used $(p_1, q_1) = (0.2, 0.9)$ and $(p_2, q_2) = (0.8, 0.25)$. Figure 4 uses $(p_1, q_1) = (0.7, 0.8)$ and $(p_2, q_2) = (0.8, 0.25)$. The first state of the sequences sampled according to the stationary distribution of the Markov chain given by $\pi_k = \frac{1}{p_k + q_k} (q_k, p_k)$ (see e.g., [44]). The sequences have a fixed length of $T = 32$.

Architecture. We considered a GPT-2-like architecture [56] using the GPT-Neo implementation [4] using local-attention suggested by [44] to improve convergence on Markov chain data (with window size of 5). The model has a hidden size of 64, 2 layers of transformer blocks with 2-heads attention. LoRA adapters for the MLE baseline have rank $r = 64$, $\alpha = 64$, and dropout disabled. To align the numbers of parameters when $K = 2$, we used $r = 32$ (and $\alpha = 32$) for LoRA-MCL. The models have a total of 65,536 trainable parameters over a total of 230,912. Note that aligning the ranks of LoRA-MCL and LoRA-MLE leads to the same conclusions. Weights of the base model were kept frozen (both for LoRA-MLE and LoRA-MCL) to mimic the dynamics on larger language models.

Training details. We used a cosine scheduler with learning rate of $1e - 4$, weight decay of $1e - 3$ with AdamW optimizer, with $(\beta_1, \beta_2) = (0.9, 0.95)$ as in [44]. We used a batch size of 128, and

trained for 500 iterations, with validation loss computed every 10 steps. Only the first 450 iterations are plotted in the Figures 1 and 4. For the LoRA-MCL runs, we trained with vanilla Winner-Takes-All update. Figure 1 (left) shows the mean and standard deviation of the Winner-Takes-All validation loss across three training seeds, for $K = 1$ (LoRA-MLE) and $K = 2$ (LoRA-MCL).

Theoretical quantities computations To verify the theoretical results, we computed the following quantities:

- **Theoretical Optimal Loss of the MLE model.** It is expressed as $\mathcal{H}(x)$ where $x \sim \frac{1}{K} \sum_{k=1}^K p(x|z_k)$. It can be approximated by Monte-Carlo sampling with samples $(z_s, x_s) \sim p(x, z)$ by first sampling modes $z_s \sim \mathcal{U}\{1, \dots, K\}$, then $x_s | z_s \sim p(x | z_s)$, and by computing

$$-\frac{1}{N} \sum_{s=1}^N \sum_{t=2}^T \log (P_s)_{x_{s,t}, x_{s,t+1}} . \quad (22)$$

Here, $(P_s)_{x_{s,t}, x_{s,t+1}}$ denotes the entry of P_s at row $x_{s,t}$ and column $x_{s,t+1}$, and N is the total number of samples. We used $N = 50,000$ here. Note that the term corresponding to $t = 1$ in (22) is discarded, as the first token is typically excluded from the loss computation. For the illustration, (22) was normalized by $T - 1$, since the first token is discarded.

- **Theoretical Optimal Loss of the MCL model.** It is computed by subtracting $\log K$ to the Theoretical optimal loss (22) of the MLE model. To verify (iii) in Proposition 1, we also computed the mixture of entropy rates given by (11), using a normalization factor of $T - 1$.

E Experimental details on the Audio and Image Captioning tasks

E.1 Setup

Dataset statistics are provided in Table 4.

Audio Datasets. We conducted experiments on two audio captioning datasets: Clotho-V2 [14, 10] and AudioCaps [16, 30]. For both datasets, we used the official training, validation, and test splits. Clotho-V2 provides five reference captions per audio clip across all splits, whereas AudioCaps includes a single caption per clip in the training set and five captions per clip in the validation and test sets. During training on Clotho-V2, which is performed on 10 epochs, at each epoch, one of the five reference captions is sampled uniformly at random for each audio clip.

Vision datasets. We conducted experiments on the TextCaps dataset. Specifically, we used the official training split for training and the official validation split as our test set. Since each image in the dataset is annotated with five different captions, we duplicated each image five times—associating each duplicate with a distinct caption—to ensure that all reference captions are seen during a single training epoch.

Preprocessing of audio data. Following the implementation of [31], for Clotho and AudioCaps raw audio files are resampled from 44.1 kHz and 32 kHz respectively to 16 kHz. They are then cropped to a maximum length of 30 seconds for Clotho and 10 seconds for AudioCaps. The data is then fed to the Qwen-2-Audio pipeline, which includes conversion of the raw waveform into a 128-channel mel-spectrogram, with a window size of 25 ms and a hop size of 10 ms.

Preprocessing of image data. Our image pre-processing pipeline follows the recipe of LLaVA (i.e., resizing to (336, 336) and normalization using CLIP mean and standard deviation).

For both modalities, we used the HuggingFace transformers [78] and PEFT [46] Python libraries as part of the implementation. Note that for each of the experiments, we set the repetition penalty [29] to 1.1 for decoding.

E.2 Audio Captioning Experiments

E.2.1 Experimental setup

Architecture and training. We used the Instructed version of Qwen-2-Audio [6] as the base model, which features ~ 8.4 billion parameters. We trained using bfloat16 precision. We used LoRA

Table 4: **Statistics of the audio and image captioning datasets.** Num. samples includes {train, validation, test} sets, except for AudioCaps, where we used only {train, validation} sets.

Dataset	Num. samples	Duration (h)	Num. Captions	Modality
AudioCaps [30]	48,286	134.1	54 K	Audio
Clotho [10]	5,929	37.0	30 K	Audio
TextCaps [65]	25,119	N/A	126 K	Image

adapters applied to the Q, K, V linear projections of the attention modules, and the upside and downside projections of the feedforward blocks, for all the transformer blocks, which include both the audio encoder and language model decoder. We used a rank r , with $r = \alpha = 8$ unless otherwise stated, with dropout equal to 0.1. We trained with a batch size of 2, with AdamW optimizer [40] (with $\beta_1 = 0.9$, and $\beta_2 = 0.98$), weight decay of 0.05, using a cosine scheduler with minimum learning rate of 10^{-6} and maximum learning rate of 10^{-5} , with a warmup ratio of 0.1. Gradient clipping is used with a maximum gradient norm of 1.0. The validation loss was computed once every epoch.

E.2.2 Additional results

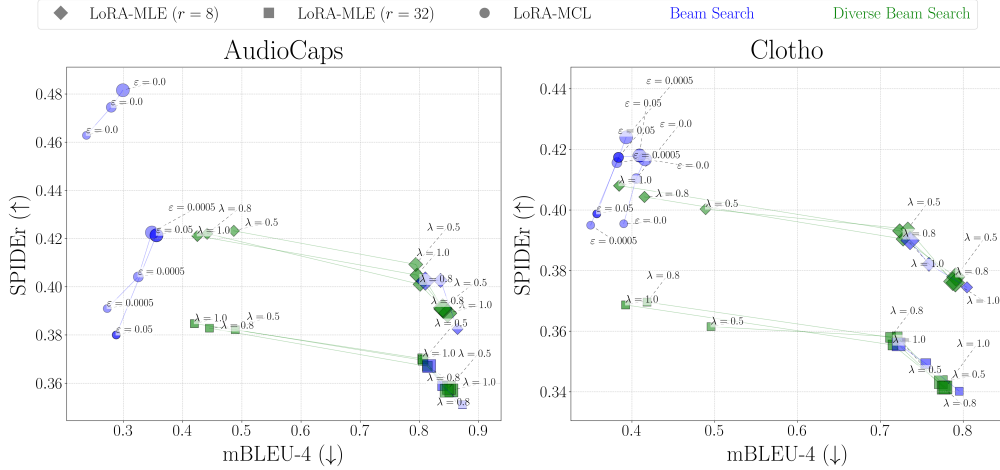


Figure 5: **Quality vs. Diversity on Audio Captioning with 4 candidates.**

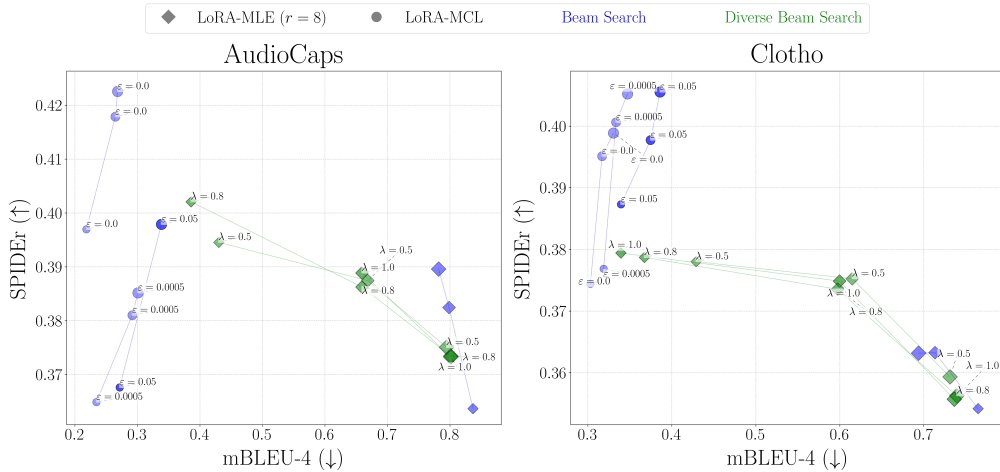


Figure 6: **Quality vs. Diversity on Audio Captioning with 3 candidates.**

Table 5: **Results on Clotho-V2 with 5 candidates and MAP Decoding.** ‘BS’ and ‘DBS’ stand for beam search and diverse beam search respectively.

Training	Decoding	Beam	Div1	Div2	mBLEU-4	BLEU-1	BLEU-4	METEOR	ROUGE-L	sBERT	CIDEr-D	SPICE	SPIDEr
LoRA-MLE ($r = 8$)	BS	5	0.298	0.360	0.827	0.651	0.133	0.229	0.443	0.575	0.621	0.175	0.391
LoRA-MLE ($r = 40$)	BS	5	0.300	0.365	0.819	0.619	0.105	0.213	0.422	0.559	0.556	0.166	0.354
LoRA-MLE ($r = 8$)	BS	10	0.310	0.386	0.787	0.650	0.139	0.233	0.450	0.576	0.634	0.181	0.400
LoRA-MLE ($r = 40$)	BS	10	0.314	0.393	0.780	0.623	0.113	0.219	0.426	0.561	0.564	0.170	0.360
LoRA-MLE ($r = 8$)	BS	25	0.316	0.402	0.764	0.653	0.143	0.236	0.453	0.580	0.639	0.184	0.404
LoRA-MLE ($r = 40$)	BS	25	0.324	0.411	0.750	0.629	0.121	0.222	0.433	0.563	0.580	0.171	0.368
LoRA-MLE ($r = 8$)	DBS ($\lambda = 0.5$)	5	0.421	0.560	0.524	0.679	0.145	0.241	0.467	0.597	0.674	0.193	0.421
LoRA-MLE ($r = 40$)	DBS ($\lambda = 0.5$)	5	0.422	0.558	0.524	0.652	0.122	0.224	0.445	0.582	0.601	0.176	0.378
LoRA-MLE ($r = 8$)	DBS ($\lambda = 0.8$)	5	0.451	0.606	0.446	0.683	0.149	0.242	0.470	0.600	0.678	0.194	0.423
LoRA-MLE ($r = 40$)	DBS ($\lambda = 0.8$)	5	0.454	0.607	0.444	0.659	0.125	0.227	0.450	0.585	0.612	0.179	0.384
LoRA-MLE ($r = 8$)	DBS ($\lambda = 1.0$)	5	0.466	0.627	0.413	0.685	0.147	0.243	0.471	0.602	0.683	0.195	0.426
LoRA-MLE ($r = 40$)	DBS ($\lambda = 1.0$)	5	0.470	<u>0.628</u>	0.414	0.660	0.124	0.228	0.451	0.588	0.614	0.180	0.386
LoRA-MLE ($r = 8$)	DBS ($\lambda = 0.5$)	10	0.376	0.475	0.722	0.667	0.139	0.238	0.459	0.593	0.656	0.190	0.413
LoRA-MLE ($r = 40$)	DBS ($\lambda = 0.5$)	10	0.377	0.480	0.716	0.642	0.115	0.223	0.439	0.575	0.589	0.179	0.374
LoRA-MLE ($r = 8$)	DBS ($\lambda = 0.8$)	10	0.386	0.491	0.708	0.668	0.139	0.238	0.459	0.595	0.652	0.191	0.412
LoRA-MLE ($r = 40$)	DBS ($\lambda = 0.8$)	10	0.390	0.495	0.704	0.640	0.115	0.223	0.437	0.577	0.585	0.179	0.371
LoRA-MLE ($r = 8$)	DBS ($\lambda = 1.0$)	10	0.392	0.495	0.704	0.664	0.138	0.240	0.455	0.596	0.655	0.192	0.413
LoRA-MLE ($r = 40$)	DBS ($\lambda = 1.0$)	10	0.395	0.498	0.704	0.641	0.112	0.224	0.437	0.578	0.583	0.182	0.372
LoRA-MLE ($r = 8$)	DBS ($\lambda = 0.5$)	25	0.304	0.369	0.813	0.650	0.134	0.229	0.445	0.574	0.625	0.176	0.393
LoRA-MLE ($r = 40$)	DBS ($\lambda = 0.5$)	25	0.305	0.370	0.812	0.619	0.106	0.214	0.423	0.558	0.555	0.166	0.354
LoRA-MLE ($r = 8$)	DBS ($\lambda = 0.8$)	25	0.302	0.366	0.818	0.649	0.133	0.228	0.443	0.574	0.620	0.176	0.391
LoRA-MLE ($r = 40$)	DBS ($\lambda = 0.8$)	25	0.304	0.369	0.814	0.619	0.106	0.214	0.423	0.558	0.556	0.166	0.354
LoRA-MLE ($r = 8$)	DBS ($\lambda = 1.0$)	25	0.302	0.365	0.819	0.648	0.133	0.229	0.444	0.574	0.620	0.177	0.391
LoRA-MLE ($r = 40$)	DBS ($\lambda = 1.0$)	25	0.305	0.369	0.814	0.619	0.105	0.214	0.423	0.558	0.556	0.167	0.355
LoRA-MCL ($\epsilon = 0.0$)	BS	1	0.490	0.633	0.389	0.662	0.127	0.231	0.453	0.597	0.643	0.186	0.401
LoRA-MCL ($\epsilon = 0.0005$)	BS	1	0.464	0.609	0.433	0.672	0.132	0.233	0.459	0.597	0.649	0.185	0.404
LoRA-MCL ($\epsilon = 0.05$)	BS	1	0.471	0.623	0.405	0.677	0.141	0.238	0.463	0.600	0.672	0.191	0.419
LoRA-MCL ($\epsilon = 0.0$)	BS	2	<u>0.477</u>	0.622	<u>0.407</u>	0.675	0.147	0.237	0.468	0.598	0.670	0.191	0.417
LoRA-MCL ($\epsilon = 0.0005$)	BS	2	0.449	0.594	0.453	0.697	0.151	0.243	0.471	0.597	0.679	0.193	0.424
LoRA-MCL ($\epsilon = 0.05$)	BS	2	0.448	0.598	0.450	0.681	<u>0.157</u>	0.246	<u>0.478</u>	0.600	0.700	0.197	0.436
LoRA-MCL ($\epsilon = 0.0$)	BS	5	0.473	0.618	0.420	0.680	0.153	0.242	0.471	0.599	0.689	0.194	0.429
LoRA-MCL ($\epsilon = 0.0005$)	BS	5	0.443	0.585	0.474	0.688	0.154	0.246	0.475	0.598	0.684	0.197	0.429
LoRA-MCL ($\epsilon = 0.05$)	BS	5	0.445	0.592	0.465	<u>0.691</u>	0.165	0.249	0.482	<u>0.601</u>	0.708	0.199	0.442

Table 6: **Results for AudioCaps with 5 candidates and MAP Decoding.**

Training	Decoding	Beam	Div1	Div2	mBLEU-4	BLEU-1	BLEU-4	METEOR	ROUGE-L	sBERT	CIDEr-D	SPICE	SPIDEr
LoRA-MLE ($r = 8$)	BS	5	0.238	0.303	0.881	0.601	0.145	0.304	0.490	0.682	0.582	0.239	0.400
LoRA-MLE ($r = 40$)	BS	5	0.232	0.298	0.888	0.576	0.134	0.296	0.472	0.679	0.510	0.234	0.362
LoRA-MLE ($r = 8$)	BS	10	0.252	0.331	0.849	0.606	0.156	0.309	0.497	0.686	0.608	0.242	0.414
LoRA-MLE ($r = 40$)	BS	10	0.246	0.324	0.861	0.581	0.147	0.300	0.479	0.681	0.520	0.238	0.369
LoRA-MLE ($r = 8$)	BS	25	0.263	0.352	0.825	0.604	0.163	0.310	0.500	0.687	0.616	0.245	0.418
LoRA-MLE ($r = 40$)	BS	25	0.258	0.350	0.830	0.583	0.156	0.304	0.483	0.685	0.531	0.240	0.373
LoRA-MLE ($r = 8$)	DBS ($\lambda = 0.2$)	5	0.312	0.454	0.684	0.620	0.166	0.317	0.508	0.697	0.622	0.257	0.421
LoRA-MLE ($r = 40$)	DBS ($\lambda = 0.2$)	5	0.310	0.462	0.676	0.595	0.157	0.314	0.492	0.697	0.534	0.255	0.376
LoRA-MLE ($r = 8$)	DBS ($\lambda = 0.5$)	5	0.358	0.545	0.531	0.636	0.188	0.327	0.521	0.707	0.664	0.270	0.445
LoRA-MLE ($r = 40$)	DBS ($\lambda = 0.5$)	5	0.354	0.551	0.528	0.610	0.183	0.324	0.506	0.707	0.577	0.267	0.400
LoRA-MLE ($r = 8$)	DBS ($\lambda = 0.8$)	5	0.377	0.576	0.483	0.640	0.193	0.330	0.521	0.708	0.672	0.270	0.447
LoRA-MLE ($r = 40$)	DBS ($\lambda = 0.8$)	5	0.374	0.585	0.473	0.614	0.185	0.324	0.509	0.708	0.588	0.269	0.405
LoRA-MLE ($r = 8$)	DBS ($\lambda = 1.0$)	5	0.386	0.590	0.460	0.638	0.190	0.329	0.521	0.709	0.668	0.269	0.444
LoRA-MLE ($r = 40$)	DBS ($\lambda = 1.0$)	5	0.382	0.598	0.452	0.612	0.181	0.323	0.505	0.709	0.581	0.266	0.401
LoRA-MLE ($r = 8$)	DBS ($\lambda = 0.5$)	10	0.314	0.439	0.777	0.624	0.180	0.318	0.510	0.699	0.636	0.262	0.431
LoRA-MLE ($r = 40$)	DBS ($\lambda = 0.5$)	10	0.309	0.440	0.780	0.605	0.170	0.315	0.496	0.699	0.558	0.260	0.390
LoRA-MLE ($r = 8$)	DBS ($\lambda = 0.8$)	10	0.320	0.448	0.770	0.624	0.176	0.318	0.507	0.700	0.626	0.263	0.426
LoRA-MLE ($r = 40$)	DBS ($\lambda = 0.8$)	10	0.316	0.451	0.771	0.604	0.167	0.313	0.496	0.698	0.556	0.258	0.388
LoRA-MLE ($r = 8$)	DBS ($\lambda = 1.0$)	10	0.325	0.455	0.764	0.621	0.175	0.317	0.506	0.702	0.632	0.262	0.427
LoRA-MLE ($r = 40$)	DBS ($\lambda = 1.0$)	10	0.322	0.456	0.769	0.602	0.165	0.313	0.495	0.699	0.553	0.258	0.386
LoRA-MLE ($r = 8$)	DBS ($\lambda = 0.5$)	25	0.247	0.319	0.864	0.604	0.152	0.306	0.493	0.682	0.597	0.243	0.408
LoRA-MLE ($r = 40$)	DBS ($\lambda = 0.5$)	25	0.241	0.315	0.872	0.582	0.141	0.298	0.477	0.683	0.523	0.236	0.370
LoRA-MLE ($r = 8$)	DBS ($\lambda = 0.8$)	25	0.246	0.316	0.867	0.603	0.148	0.305	0.492	0.682	0.592	0.242	0.406
LoRA-MLE ($r = 40$)	DBS ($\lambda = 0.8$)	25	0.240	0.311	0.876	0.581	0.138	0.298	0.475	0.682	0.523	0.235	0.369
LoRA-MLE ($r = 8$)	DBS ($\lambda = 1.0$)	25	0.245	0.314	0.870	0.603	0.150	0.306	0.493	0.682	0.592	0.242	0.406
LoRA-MLE ($r = 40$)	DBS ($\lambda = 1.0$)	25	0.239	0.310	0.878	0.581	0.140	0.298	0.476	0.682	0.525	0.236	0.370
LoRA-MCL ($\epsilon = 0.0$)	BS	1	0.496	0.707	0.211	0.649	0.174	0.323	0.518	0.702	0.648	0.255	0.428
LoRA-MCL ($\epsilon = 0.0005$)	BS	1	0.450	<u>0.678</u>	0.292	0.654	0.195	0.333	0.530	0.710	0.679	0.272	0.448
LoRA-MCL ($\epsilon = 0.05$)	BS	1	0.438	0.663	0.326	0.640	0.198	0.332	0.517	0.710	0.611	0.272	0.414
LoRA-MCL ($\epsilon = 0.0$)	BS	2	0.459	0.672	<u>0.233</u>	0.650	0.196	0.330	0.529	0.702	0.679	0.262	0.447
LoRA-MCL ($\epsilon = 0.0005$)	BS	2	0.408	0.629	0.348	0.658	0.213	0.336	0.539	<u>0.711</u>	<u>0.716</u>	0.276	0.470
LoRA-MCL ($\epsilon = 0.05$)	BS	2	0.397	0.616	0.384	0.632	0.208	0.336	0.524	0.710	0.629	0.274	0.424
LoRA-MCL ($\epsilon = 0.0$)	BS	5	0.453	0.657	0.254	0.656	0.211	0.331	0.532	0.702	0.697	0.262	0.456
LoRA-MCL ($\epsilon = 0.0005$)	BS	5	0.403	0.615	0.372	0.661	0.229	0.339	0.545	0.712	0.744	0.278	0.484
LoRA-MCL ($\epsilon = 0.05$)	BS	5	0.392	0.599	0.419	0.640	<u>0.221</u>	<u>0.337</u>	0.530	0.710	0.660	0.274	0.442

Varying the number K of hypotheses. Figures 5 and 6 present the same scatter plots as Figure 2, but with 4 and 3 candidates respectively. The observed trends remain consistent: LoRA-MCL continues to demonstrate an excellent balance between quality and diversity. Notably, the case with $\epsilon = 0$ performs particularly well, which we attribute to improved stability in vanilla WTA when the number of heads is reduced. Note that the detailed results with $K = 5$ associated with Figure 2 are given in Tables 5 and 6 for Clotho and AudioCaps, respectively.

Evaluating with Sampling-based decoding. We also report results using sampling-based decoding methods in Tables 7 and 8 for Clotho and AudioCaps. Specifically, we use Top- k sampling with $k = 50$, Top- p sampling with $p = 0.95$, and Typical sampling with a threshold of 0.95. For all

Table 7: Results for Clotho with 5 candidates and Sampling-based decoding.

Training	Decoding	Div1	Div2	mBLEU-4	BLEU-1	BLEU-4	METEOR	ROUGE-L	sBERT	CIDEr-D	SPICE	SPIDEr
LoRA-MLE ($r = 8$)	Top- k sampling	0.635	0.814	0.113	0.585	0.073	0.214	0.400	0.590	0.486	0.176	0.315
LoRA-MLE ($r = 8$)	Typical p sampling	0.645	<u>0.817</u>	0.108	0.589	0.077	0.215	0.402	0.587	0.492	<u>0.177</u>	0.319
LoRA-MLE ($r = 8$)	Nucleus (Top- p) sampling	0.646	0.818	0.106	0.592	0.074	0.214	0.401	<u>0.589</u>	0.489	0.178	0.318
LoRA-MCL ($\varepsilon = 0.0005$)	Top- k sampling	0.642	0.816	0.110	0.600	0.079	0.214	0.406	0.588	0.500	0.175	0.322
LoRA-MCL ($\varepsilon = 0.0005$)	Typical p sampling	<u>0.648</u>	0.815	0.111	<u>0.595</u>	0.082	<u>0.215</u>	0.409	0.584	0.506	0.175	0.327
LoRA-MCL ($\varepsilon = 0.0005$)	Nucleus (Top- p) sampling	0.649	0.817	<u>0.107</u>	0.595	<u>0.079</u>	0.214	<u>0.408</u>	0.586	<u>0.504</u>	0.171	<u>0.325</u>

Table 8: Results for AudioCaps with 5 candidates and Sampling-based decoding.

Training	Decoding	Div1	Div2	mBLEU-4	BLEU-1	BLEU-4	METEOR	ROUGE-L	sBERT	CIDEr-D	SPICE	SPIDEr
LoRA-MLE ($r = 8$)	Top- k sampling	0.562	0.810	0.134	0.560	0.115	0.299	0.457	0.699	0.442	0.241	0.318
LoRA-MLE ($r = 8$)	Nucleus (Top- p) sampling	0.576	0.810	0.141	0.560	0.121	<u>0.299</u>	0.460	0.699	0.450	0.241	0.325
LoRA-MLE ($r = 8$)	Typical sampling	0.567	0.809	0.143	0.550	0.115	0.300	0.452	0.697	0.390	0.241	0.294
LoRA-MCL ($\varepsilon = 0.0005$)	Top- k sampling	0.583	0.830	0.098	0.582	0.115	0.298	0.470	0.700	0.498	0.239	0.344
LoRA-MCL ($\varepsilon = 0.0005$)	Nucleus (Top- p) sampling	<u>0.597</u>	<u>0.831</u>	0.098	0.575	0.124	0.298	<u>0.468</u>	0.697	0.497	0.237	<u>0.344</u>
LoRA-MCL ($\varepsilon = 0.0005$)	Typical sampling	0.597	0.831	<u>0.098</u>	<u>0.575</u>	<u>0.124</u>	0.298	0.468	0.697	<u>0.497</u>	0.237	0.344

sampling methods, we apply a repetition penalty of 1.1, following [29]. In these experiments, the temperature was set to $\eta = 1.0$.

We observe that both LoRA-MLE and LoRA-MCL yield significantly higher diversity compared to MAP decoding, albeit at the cost of reduced output quality. This trade-off is evident when comparing results in Tables 5 and 6. While both methods show an overall improvement in quality on the CIDEr and SPIDEr metrics across datasets, performance on other metrics such as METEOR and SPICE remains relatively comparable. In terms of diversity, there does not appear to be a clear trend indicating which method performs best, as the conclusions vary depending on the dataset. These findings suggest the need for further evaluation with different values of epsilon to better understand the quality-diversity trade-off in sampling-based decoding. Additionally, a more in-depth exploration of how the number of generated hypotheses affects sampling quality—and its implications for test-time inference scaling with LoRA-MCL [85]—is left for future work.

E.3 Image Captioning Experiments

E.3.1 Experimental setup

Table 9: Quality and Diversity Evaluation on TextCaps with 3 candidates. For each of the presented metrics, higher is better (\uparrow) except for mBLEU-4 (\downarrow). LoRA-MCL is trained with $\varepsilon = 0.1$, $r = 8$ and $\alpha = 32$. LoRA-MLE is trained with $r = 24$ and $\alpha = 96$. For completeness, we also trained LoRA-MLE with $r = 8$ and $\alpha = 32$ in the rows marked with \dagger .

Training	Decoding	Beam	Div1	Div2	mBLEU-4	BLEU-1	BLEU-4	METEOR	ROUGE-L	sBERT	CIDEr-D	SPICE	SPIDEr
LoRA-MLE	Beam Search	3	0.433	0.509	0.688	0.802	0.318	0.315	0.580	0.670	1.517	0.244	0.873
LoRA-MLE †	Beam Search	3	0.383	0.421	0.833	0.788	0.315	0.317	0.573	0.670	1.517	0.241	0.874
LoRA-MLE	Beam Search	6	0.402	0.457	0.786	0.795	0.338	0.326	0.583	0.671	1.557	0.246	0.895
LoRA-MLE †	Beam Search	6	0.401	0.456	0.784	0.796	0.339	0.327	0.585	0.672	1.572	0.248	0.903
LoRA-MLE	DBS ($\lambda = 0.5$)	3	0.489	0.600	0.529	0.818	0.345	0.325	0.596	0.684	1.571	0.253	0.902
LoRA-MLE	DBS ($\lambda = 0.8$)	3	0.530	0.655	0.437	0.824	0.349	0.327	<u>0.601</u>	0.686	1.590	0.251	0.909
LoRA-MLE	DBS ($\lambda = 1.0$)	3	0.540	0.669	0.416	0.822	0.348	0.326	0.599	0.685	1.586	0.250	0.906
LoRA-MLE †	DBS ($\lambda = 0.5$)	3	0.485	0.597	0.531	0.821	0.346	0.326	0.596	0.685	1.589	0.255	0.912
LoRA-MLE †	DBS ($\lambda = 0.8$)	3	0.485	0.597	0.531	0.821	0.346	0.326	0.596	0.685	1.589	0.255	0.912
LoRA-MLE †	DBS ($\lambda = 1.0$)	3	<u>0.535</u>	<u>0.665</u>	<u>0.425</u>	<u>0.827</u>	<u>0.357</u>	0.327	0.601	0.686	1.601	0.252	0.915
LoRA-MLE	DBS ($\lambda = 0.5$)	6	0.455	0.532	0.694	0.813	0.344	0.328	0.595	0.681	1.580	0.253	0.908
LoRA-MLE	DBS ($\lambda = 0.8$)	6	0.470	0.549	0.671	0.812	0.341	0.328	0.593	0.681	1.573	0.251	0.903
LoRA-MLE	DBS ($\lambda = 1.0$)	6	0.474	0.553	0.666	0.812	0.340	0.328	0.592	0.680	1.577	0.250	0.904
LoRA-MLE †	DBS ($\lambda = 0.5$)	6	0.451	0.528	0.697	0.808	0.343	0.329	0.594	0.681	1.586	0.253	0.911
LoRA-MLE †	DBS ($\lambda = 0.8$)	6	0.464	0.542	0.681	0.810	0.340	0.329	0.593	0.680	1.583	0.253	0.909
LoRA-MLE †	DBS ($\lambda = 1.0$)	6	0.473	0.551	0.671	0.810	0.341	0.328	0.592	0.680	1.584	0.251	0.908
LoRA-MCL	Beam Search	1	0.499	0.599	0.520	0.828	0.344	<u>0.330</u>	0.597	0.690	1.674	<u>0.255</u>	0.955
LoRA-MCL	Beam Search	2	0.507	0.618	0.490	0.824	0.360	0.333	0.604	<u>0.687</u>	<u>1.627</u>	0.258	<u>0.932</u>

We used LLaVA 1.6 as the base model, which features 7.1 billion parameters. We trained using bfloat16 precision. We used LoRA adapters applied to the Q , K , V , up and down linear projections of each block of the language model. We used a rank r , with $r = 8$ and $\alpha = 32$ unless otherwise stated, with dropout equal to 0.1. We trained each model with a batch size of 8, with AdamW

optimizer [40] (with $\beta_1 = 0.9$, and $\beta_2 = 0.98$), weight decay of 0.05, using a cosine scheduler with maximum learning rate of 10^{-4} , with a warmup ratio of 0.1. Gradient clipping is used with a maximum gradient norm of 1.0. We used 1 epoch for training, where we duplicated the image as many times as the number of its captions, such that the model sees exactly one time each caption.

E.4 Additional results

Table 9 presents the results of LoRA-MCL and LoRA-MLE. Almost all the metrics show the same trend in which LoRA-MCL outperforms LoRA-MLE with Beam Search (BS) and Diverse Beam Search (DBS) in terms of quality, although DBS produces more varied outputs. Depending on the rank ($r = 8$ or $r = 24$), we found that setting $\lambda = 1.0$ or $\lambda = 0.8$, respectively, yields the best quality scores for DBS. Similar to our experiments on Audio Captioning, increasing the rank of LoRA-MLE results in a slight degradation in performance but improves diversity. Additionally, increasing the number of beams in BS with LoRA-MLE results in slightly improved performance but reduced diversity. In contrast, increasing the number of beams in DBS with LoRA-MLE (with fixed λ) leads to declines in both quality and diversity. Interestingly, with LoRA-MCL, increasing the number of beams enhances both performance and diversity here.

E.4.1 Artificial multilingual dataset creation

To evaluate the behaviour of LoRA-MCL under a multi-modal distribution, we simulated an artificial bi-modal dataset by automatically translating half of the captions from English to French using T5-small [57], while keeping the prompts in English. More specifically, we randomly sampled half of the images and translated their five associated captions. All the training parameters are the same as those in the experiments on the original TextCaps dataset, except the learning rate, which we set at 2×10^{-5} (as the maximum value in the scheduler) in both the LoRA-MLE and LoRA-MCL.

During evaluation, to assess which head is considered as the winner (for the head specialization analysis), we selected the one that maximizes the SPIDeR score over the references of the given sample.

E.5 Computation details

We run the experiments mostly on H100 NVIDIA GPUs with 80 GB of RAM. Trainings and inferences were launched on a single GPU for the Audio Captioning experiments, and up to 8 GPUs for the Image Captioning experiments. The total computing resources used for this project, including failed experiments, amount to approximately 20,000 GPU hours.